

**SEMELWEIS EGYETEM
DOKTORI ISKOLA**

Ph.D. értekezések

2526.

NÉMETH ORSOLYA

**Szemészet
című program**

Programvezető: Dr. Nagy Zoltán Zsolt, egyetemi tanár
Témavezető: Dr. Szentmáry Nóra, kutatóprofesszor

Ocular surface thermography in keratoconus and keratoglobus patients

PhD Thesis

Orsolya Németh M.D.

Clinical Medicine Doctoral School

Semmelweis University



Supervisor:

Nóra Szentmáry, M.D., Ph.D.

Official reviewers:

Péter Vámosi, M.D., Ph.D.

Antal Szabó M.D., Ph.D.

Head of the Complex Examination Committee:

László Smeller, M.D., Ph.D., D.Sc.

Members of the Complex Examination Committee:

Ágnes Kerényi, M.D., Ph.D.

Miklós Resch M.D., Ph.D.

Budapest

2020

Table of contents

1. List of abbreviations.....	4
2. Introduction	6
2.2 Keratoconus.....	6
2.3 Keratoglobus	8
2.4 Thermography	9
2.5 Endothelial cell layer	11
3. Objectives	12
4. Results.....	13
4.1 Ocular Surface Disease Index and ocular thermography in keratoconus patients.....	13
4.2 Correlation between corneal endothelial cell density and central corneal temperature in normal and keratoconus eyes	19
4.3 Ocular Surface Disease Index, biomechanical properties and ocular thermography in a keratoglobus patient	24
5. Discussion	30
5.1 Ocular Surface Disease Index and ocular thermography in keratoconus patients.....	30
5.2 Correlation between corneal endothelial cell density and central corneal temperature in normal and keratoconus eyes	32
5.3 Ocular Surface Disease Index, biomechanical properties and ocular thermography in a keratoglobus patient	35
6. Conclusions	38
7. Summary	39
8. References.....	40
9. Bibliography.....	49
10. Acknowledgements	51

1. List of abbreviations

6A - hexagonality

ARTh - Ambrosio relational thickness to the horizontal profile

AS-OCT - anterior segment optical coherence tomography

BCVA – best corrected visual acuity

BSA - corneal back surface area at a central 5 mm region

CCT – central corneal thickness

CKI - centre keratoconus index

CYL - topographic cylinder

CV – coefficient of variation of corneal endothelial area

DA - deformation amplitude ratio

ECD – endothelial cell density

FSA - corneal front surface area at a central 5 mm region

IHA - index of height asymmetry

IHD - index of height decentration

IR - integrated radius

ISV - index of surface variance

IVA - index of vertical asymmetry

KC – keratoconus

KCI - Klyce/Maeda keratoconus index

KI - keratoconus index

KPI - keratoconus prediction index

KSI - Smolek/Klyce keratoconus severity index

OST – ocular surface temperature

PCA – pachymetry at the apex of the cone

PCP – pachymetry at the pupillary centre

PKP – penetrating keratoplasty

PMD – pellucid marginal degeneration

RmB – corneal back surface radius of curvature

RmF – corneal front surface radius of curvature

SAI - surface asymmetry index

SPA1 - stiffness parameter at applanation 1

SRI - surface regularity index

TKC – topographic keratoconus classification

UCVA – uncorrected visual acuity

2. Introduction

The cornea is the “windshield” of the eye. Therefore, its clarity and regularity is necessary for good vision. Keratoconus and keratoglobus are ectatic corneal diseases, characterized by bilateral, progressive corneal thinning and protrusion (Garcia-Ferrer et al 2019). The etiology of corneal ectatic diseases still remains unknown. Genetical factors, eye rubbing, atopic disease, vernal keratoconjunctivitis, dry eye disease, hay fever, asthma could all be associated with the development of ectatic corneal diseases (Chang et al, 2013; Kenney MC et al, 2003; Pásztor D et al, 2016; Weed KH et al, 2008). Although keratoconus and keratoglobus are defined as noninflammatory corneal diseases, several studies discuss their potential inflammatory origin (Lema I et al, 2009; Kolozsvári BL et al, 2014).

2.1 Keratoconus

Keratoconus (KC) was first described in 1854 (Nottingham 1984). It is the most common corneal ectasia, characterised by bilateral, asymmetric corneal degeneration, which leads to thinning and protrusion of the cornea (Kennedy et al, 1986). This corneal protrusion results in high myopia and astigmatism, affecting visual quality (Kennedy et al, 1986). The protrusion usually becomes apparent in the second decade of life, typically progresses until the fourth decade, and then stabilises (Rabinowitz 1998). Its prevalence is approximately 1:2000 in the Caucasian population, but its exact aetiology remains unknown. Although KC cases are sporadic, some studies have reported autosomal dominant or recessive inheritance (Chang et al. 2013). Eye rubbing may be the most important environmental factor related to the development of KC. Therefore, patients with a history of atopy may have a higher risk of developing KC (Weed et al, 2008). Although KC is defined as a “non-inflammatory” corneal disease, several studies have reported a potential inflammatory origin. For example, proinflammatory cytokines IL-6, IL-1 β , IFN- γ , and TNF- α could be measured in the tear film of KC patients (Lema et al, 2009; Kolozsvári et al, 2014; Pásztor et al, 2016).

Several biochemical theories have been proposed to explain corneal thinning resulting from the loss of corneal structural components. Määttä et al. previously reported

differences in collagen XIII (Määttä et al, 2006), XV, and XVIII between corneas from normal individuals and KC patients (Määttä et al, 2006). Excessive degradation of the corneal stroma, as commonly observed in KC, may be caused by proteolytic enzyme activity due to increased levels of proteases and other catabolic enzymes (Fukuchi et al, 1994). Keratocytes in the corneas of KC patients have 4-times as many interleukin (IL)-1 receptors as corneas in healthy individuals (Bereau et al, 1993). According to Stachon et al. (Stachon et al, 2017), in the aqueous humour of KC patients, urea and prolactin are decreased and free tiroxin (fT4) increased, whereas the uric acid concentration remains unchanged. The urea cycle plays an important role in stable collagen synthesis through hydroxyproline production, which is responsible for collagen stabilisation. Stachon et al. identified suppressed arginase activity in cultured KC keratocytes, which leads to a lower urea level in the cells (Stachon et al, 2017). Microtraumas, such as eye rubbing because of atopy or contact lens wear, cause higher IL-1 release (Bron et al, 1996). These mechanical injuries result in oxidative stress in the cornea, which could have an effect on KC development (Kenney et al, 2003). A key gene in inflammatory processes is nuclear factor kappa B (NF-κB), a transcription factor for the enzyme nitric oxide synthase (NOS). NOS is involved in inflammatory processes with the competing enzyme arginase (Stachon et al, 2019). Stachon et al. (Stachon et al, 2019) found increased expression of NF-κB and iNOS in KC keratocytes. Thus, the altered metabolic activity suggests that KC may be caused by inflammatory processes. (Németh et al, 2020a)

In KC patients, ocular surface disease is characterized by worse tear quality, significantly lower break-up time (BUT), and higher fluorescein and rose bengal staining scores than the normal population (Dogru et al, 2013). A correlation between ocular surface disease and KC stage has also been verified (Dogru et al, 2003). Although, some of the KC screening indices are also sensitive to dry eye syndrome (De Paiva et al, 2003), no interaction between measures of dry eye syndrome and topographic/tomographic changes in KC patients could be shown (Zemova et al, 2014, Németh et al 2000a). The Ocular Surface Disease Index (OSDI) questionnaire is widely used for investigation of ocular surface disease (Walt J 2004). Mathews et al. (Mathews et al, 2013) described, beside a total OSDI score, a vision-related subscore (derived from questions about vision and task performance: driving, computer use) and a discomfort-related subscore (derived from questions about ocular surface discomfort: light sensitivity; pain or grittiness or

discomfort in dry or windy environments). In keratoconus, Dienes et al. (Dienes et al. 2015) described a significantly decreased tear secretion and significantly higher OSDI scores, compared to healthy controls. Beside structural changes, innervation changes may play a role in the impaired tear secretion and the abnormal ocular sensations experienced by keratoconus patients.

2.2 Keratoglobus

Keratoglobus was first described as ectatic corneal disease in 1947 by Verrey as a distinct clinical entity (Verrey 1947). Before his description, literature did not differentiate between megalocornea, congenital glaucoma and keratoglobus. The exact etiology of keratoglobus remains unknown, although various theories describe its potential relationship with other ectatic corneal diseases such as keratoconus and pellucid marginal degeneration (Cameron 1993; Baillif et al, 2005). It is still not clarified, whether these three ectatic corneal diseases are separate or related clinical entities. Keratoglobus was first described as a congenital disorder, but up to now acquired forms have also been described (Pouliquen et al, 1985). Although its exact genetical background is not known, it is assumed to have autosomal recessive inheritance (Pouliquen et al, 1985). It has also been associated with disorders of the connective tissues such as Ehlers–Danlos syndrome (Cameron 1993), Marfan syndrome (Gregoratos et al, 1971) and Rubinstein–Taybi syndrome (Nelson and Talbot, 1989) and also to Leber congenital amaurosis (Koenekoop 2004). Secondary, acquired forms of keratoglobus have been described associated with vernal keratoconjunctivitis, chronic marginal blepharitis, idiopathic orbital inflammation (Cameron 1993) and dysthyroid eye disease (Jacobs et al, 1974).

Keratoglobus is principally characterised by a globular protrusion of the corneal tissue, associated with its diffuse thinning from limbus to limbus. (Németh et al, 2020c) The corneal thinning reaches its maximum at the corneal periphery, sometimes with one-fifth of the normal corneal thickness (Wallang and Das, 2013). Corneal diameter remains normal (Wallang and Das, 2013), which supports its differentiation from megalocornea and buphthalmos. Most interestingly, Vogt striae and Fleischer's rings are not associated with keratoglobus (Baillif et al, 2005). Patients usually present with blurred vision as a

result of the thinning and protrusion. There is high myopia with irregular astigmatism, as the main cause of poor vision in these patients, which is difficult to treat (Wallang and Das, 2013). Owing to extreme thinning and fragility of the cornea, many cases may initially present with corneal perforations, either spontaneous or following minimal trauma (Baillif 2005).

Keratoglobus is usually diagnosed by slitlamp examination, corneal topo-and tomography. Besides, anterior segment optical coherence tomography (for example the Casia-2 anterior segment optical coherence tomographer (Tomey, Erlangen-Tennenlohe, Germany) and biomechanical measurement (CorVis ST (Corneal VisualizationScheimpflug Technology, Oculus Optikgeräte GmbH, Wetzlar, Germany) may support our work in its differential diagnosis (Németh et al, 2020c).

The Casia-2 uses fourier domain technology, 1310 nm wavelength, which enables a measurement from the anterior part of the cornea to the posterior part of the lens, within one scan. Its scanning depth is approximately 13 mm, its axial resolution 10 µm and horizontal resolution 30 µm, working with a scanning speed of 50 000 A scans/second (Saito et al 2020). The CorVis ST records the reaction of the cornea to a defined air pulse using a high-speed Scheimpflug camera. It measures IOP, corneal thickness and the deformation response of the cornea. Corneal ectasia lead to changes in the viscoelastic properties of the cornea. These changes can be analyzed based on deviations in deformation response parameters, relative to normal eyes (Ambrosió et al, 2017).

2.3 Thermography

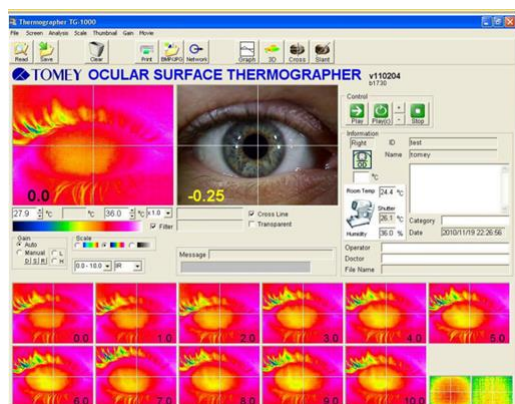


Figure 1. Ocular surface thermography in a healthy adult measured by Tomey-TG 1000 ocular surface thermographer (Tomey, Erlangen-Tennenhole, Germany)

Thermography is used in many fields of medicine (Németh et al, 2020a), including angiology (Harding 1998), oncology (Hatwar et al, 2017), and rheumatology (Lasanen et

al, 2015). Since Mapstone (Mapstone 1968, 1968, 1970) introduced infrared thermography of the ocular surface, the method has become more often used. In ophthalmology, ocular surface temperature (OST) has been investigated in ocular inflammation (Kawalii 2013), tear film abnormalities (Morgan et al, 1995), analysis of bleb function after glaucoma surgery (Kawasaki et al, 2009), after corneal refractive surgery (Betney 1997), cataract surgery (Belkin et al, 2017), and in the evaluation of ocular blood flow (Konieczka et al, 2018).

OST may be influenced by environmental and ocular factors. In the environment, changes in the ambient temperature may influence OST, but it reaches a plateau of 36°C at an ambient temperature of 40°C (Geiser et al, 2004; Kessel et al, 2010). Wind, air conditioning, or any kind of air flow affects OST through increased evaporation (Freeman and Fatt, 1973) and lower air humidity increases lacrimal evaporation (Slettedal and Ringvold 2015). Blinking interrupts corneal exposure to the environment and redistributes the tear film and its temperature (Purslow and Wolffsohn 2005).

OST also depends on ocular factors (Németh et al, 2020a; 2020b), such as the quality and quantity of the tear film and heat conduction and convection of the aqueous humour, which is determined mainly through blood flow in the ciliary body and through retrobulbar haemodynamics (Gugleta et al, 1999). As the cornea is an avascular tissue, the central corneal temperature is mainly influenced by tear film evaporation and heat convection and conduction of the aqueous humour (Gugleta et al, 1999). Nevertheless, the temperature of the peripheral cornea may also be influenced by blood flow in the perlimbal vessels (Konieczka et al, 2018).

Since the 1970s, many thermographic parameters of the eye have been described in the literature, measured under healthy or pathological conditions. The average ocular surface temperature (OST) is 32.5-36.5°C in normal healthy individuals (Pattmöller et al, 2015). Pattmöller et al. found good inter- and intra-observer reliability of the corneal surface measurements of the TG-1000 thermographer, and it yielded consistent results (Pattmöller et al, 2015). According to Moussa et al. (Moussa et al, 2013), the corneal surface temperature does not change diurnally in healthy individuals and is warmer nasally than centrally and temporally during the interblinking interval. The literature contains controversial information on the effect of corneal thickness on OST. Pattmöller

et al. (Pattmöller et al, 2015) found, that in healthy individuals, corneal thickness, endothelial cell density (ECD), and anterior chamber depth do not affect the corneal surface temperature. The corneal thickness profile appears to influence the general temperature profile, resulting in a higher temperature and lower decay in thinner corneal regions. OST has been reported to significantly decrease with increasing corneal thickness (Morgan 1994). In contrast, a progressive increase in OST from the corneal centre to the periphery has also been demonstrated by other authors (Alió et al, 1982; Efron et al, 1989).

2.4 Endothelial cell layer

The innermost layer of the cornea is the corneal endothelium, which has a single layer of flat, polygonal cells that play an essential role in maintaining stromal dehydration. Maintenance of this hydration gradient depends on tight junctions among endothelial cells and Na^+/K^+ -ATPase and bicarbonate-dependent Mg^{2+} -ATPase pump functions (Tervo et al, 1975). Adequate pump function requires a minimum number of endothelial cells. The endothelial cell density (ECD) decreases from birth ($3145\text{--}5013\text{ cells/mm}^2$) to approximately 2500 cells/mm^2 in late adulthood (Elbaz et al, 2017; Eghrari et al 2015). The vitality of the corneal endothelium is important for its barrier and pumping functions and corneal thickness is strongly associated with these characteristics (McDonald et al, 1987). A loss of corneal endothelial cell density down to several hundred cells per square millimetre generally results in corneal oedema (Reinhard et al, 2001; Langenbucher et al, 2002).

3. Objectives

Although ectatic corneal diseases are defined as noninflammatory corneal diseases, several data support the hypothesis, that these are in part of inflammatory origin.

In our studies our objectives were:

- To add insight into the relationship between ocular surface disease and KC, analysing the Ocular Surface Disease Index (OSDI) and OST in KC patients compared to controls.
- To analyse the correlation between ECD and central corneal temperature in KC patients and healthy controls.
- To describe the ocular surface disease index (OSDI), biomechanical and corneal thermographic parameters in a keratoglobus patient.

4. Results

4.1 Ocular Surface Disease Index and ocular thermography in keratoconus patients

179 eyes of 90 patients with KC (topographic KC classification [TKC] 0-1 to 4) and 82 eyes of 41 controls were examined. Participant age at the time of examination was 36.1 ± 12.5 (range 14-67) years in the KC group and 36.4 ± 12.8 (range 18-78) years in the control group ($p=0.923$). There were 34.1% females and 53.6% left eyes in the KC group, whereas the control group included 52.4% females and 47.6% left eyes. Thirty-one (38%) eyes in the control group (71% soft and 29% rigid contact lenses) and 78 (44%) eyes (all rigid contact lenses) in the KC group had previous contact lens wear. Unfortunately, we could not gather information on the number of hours with occasional/daily contact lens wear. (Németh et al, 2020a)

Best spectacle corrected visual acuity was 0.6 ± 0.3 in the KC group and 0.9 ± 0.2 in controls. The refractive cylinder was -3.5 ± 2.8 D in the KC group and -1.0 ± 1.0 D in controls. From corneal topography and tomography, surface asymmetry index (SAI), surface regularity index (SRI), Klyce/Maeda keratoconus index (KCI), Smolek/Klyce keratoconus severity index (KSI), keratoconus prediction index (KPI), index of surface variance (ISV), index of surface asymmetry (IVA), keratoconus index (KI), centre keratoconus index (CKI), index of height asymmetry (IHA), and index of height decentration (IHD) are given in **Table 1** for both groups. **Tables 2-3** provide the OSDI scores and subscores, corneal and conjunctival OST values, central corneal thickness (CCT), pachymetry at the pupillary centre (PCP), and pachymetry at the apex of the cone (PCA) in both groups. We found a significant difference in SAI, SRI, KCI, KSI, KPI, ISV, IVA, KI, CKI, IHA, IHD, CCT, PCP, and PCA between both groups ($p < 0.001$).

Table 1. Corneal topographic and tomographic data of the keratoconus patients and controls (Németh et al, 2020a).

Data are given as mean \pm SD (minimum-maximum). SAI: surface asymmetry index, SRI: surface regularity index, KCI: Klyce/Maeda keratoconus index, KSI: Smolek/Klyce neural network index, KPI: keratoconus prediction index, ISV: index of surface variance, IVA: index of vertical asymmetry, KI: keratoconus index, CKI: central keratoconus index, IHA: index of height asymmetry, IHD: index of height decentration.

A significant difference was found in all displayed topographic and tomographic data between both groups ($p<0.01$).

	SAI	SRI	KCI	KSI	KPI	ISV	IVA	KI	CKI	IHA	IHD
Keratoconus	2.1 \pm 1.6 (0.1-8.42)	1.0 \pm 0.6 (0.06-2.6)	57.0 \pm 37.2 (0-95)	50.3 \pm 29.4 (0-95)	0.35 \pm 0.1 (0.1-0.7)	84.7 \pm 49.4 (15-312)	0.9 \pm 0.5 (0.08-2.6)	1.2 \pm 0.2 (0.8-2.2)	1.1 \pm 0.1 (0.9-1.3)	26.5 \pm 22.2 (0.3-131.2)	0.1 \pm 0.1 (0.004-0.7)
Control	0.4 \pm 0.2 (0.1-1.7)	0.2 \pm 0.2 (0.0-1.2)	1.8 \pm 6.4 (0-33)	2.5 \pm 8.3 (0-45)	0.2 \pm 0.02 (0.2-0.3)	18.1 \pm 7.6 (6-44)	0.1 \pm 0.1 (0.03-0.4)	1.0 \pm 0.2 (0.9-1.09)	1.0 \pm 0.0 (0.9-1.0)	6.0 \pm 5.5 (0.1-27.8)	0.01 \pm 0.01 (0.001-0.5)
P-value	<0.01	<0.01	<0.01	<0.01	<0.01	<0.01	<0.01	<0.01	<0.01	<0.01	<0.01

Table 2. Ocular Surface Disease Index (OSDI) scores and subscores, ocular surface temperature (OST), and corneal thickness at different regions in keratoconus patients and in controls (Németh et al, 2020a).

Data are given as mean \pm SD (minimum-maximum).

VR: vision-related, DR: discomfort-related, CCT: central corneal thickness.

	OSDI	VR OSDI	DR OSDI	Central	Superior	Inferior	Nasal	Temporal	Conjunctival	CCT	Pachymetry	Pachymetry
		subscore	subscore	OST	OST	OST	OST	OST	OST		at the pupil	at the apex
Kerato-	31.5 \pm 22.0 (0-88.9)	17.7 \pm 14.6 (0-50)	14.3 \pm 10.7 (0-43.7)	34.3 \pm 0.6 (32.3-35.4)	34.2 \pm 0.6 (32.0-35.5)	34.2 \pm 0.7 (31.0-35.6)	34.2 \pm 0.6 (31.7-35.6)	34.2 \pm 0.6 (32.2-35.5)	34.5 \pm 1.0 (32.2-35.5)	475.0 \pm 50.4 (366-605)	489.6 \pm 45.5 (304-588)	480.1 \pm 51.5 (277-591)
conus												
Control	17.5 \pm 17.5 (0-79.6)	10.5 \pm 13.2 (0-50)	9.4 \pm 10.5 (0-47.5)	34.3 \pm 0.7 (31.9-35.2)	34.2 \pm 0.7 (32.1-35.2)	34.7 \pm 0.6 (32.1-35.2)	34.2 \pm 0.7 (31.9-35.3)	34.2 \pm 0.6 (32.1-35.2)	34.6 \pm 0.8 (32.1-35.2)	529.1 \pm 35.2 (463-627)	545.6 \pm 30.8 (494-637)	546.8 \pm 30.7 (494-639)
P-value	<0.001	<0.001	<0.001	0.414	0.273	0.221	0.361	0.283	0.283	<0.001	<0.001	<0.001

Table 3. Ocular Surface Disease Index (OSDI) scores and subscores, central and conjunctival ocular surface temperature (OST) in different stages of keratoconus (KC) and controls (Németh et al, 2020a).Data are given as mean \pm SD (minimum-maximum).

VR: vision-related, DR: discomfort-related.

	OSDI	VR	DR	Central	Conjunctival
		subscore	subscore	OST	OST
KC4	41.9 \pm 25.9 (0-88.9)	25.6 \pm 18.0 (0-50)	17.5 \pm 12.5 (0-37.5)	34.2 \pm 0.6 (32.9-34.9)	34.5 \pm 0.9 (32.0-35.9)
KC3	29.3 \pm 18.5 (4.2-88.9)	16.3 \pm 11.9 (0-50)	13.0 \pm 9.7 (0-43.75)	34.3 \pm 0.7 (32.3-35.3)	34.5 \pm 1.2 (31.1-36.2)
KC2	31.7 \pm 25.1 (0-87.5)	17.6 \pm 15.9 (0-50)	14.8 \pm 12.4 (2-35)	34.2 \pm 0.6 (32.3-35.3)	34.5 \pm 0.9 (30.8-36.1)
KC1	30.1 \pm 19.2 (4.2-60.4)	15.4 \pm 11.5 (0-39.5)	14.0 \pm 8.9 (0-47.5)	34.3 \pm 0.7 (32.4-35.4)	34.3 \pm 1.0 (31.9-35.8)
Control	17.5 \pm 17.5 (0-79.6)	10.5 \pm 13.2 (0-50)	9.4 \pm 10.5 (0-47.5)	34.3 \pm 0.7 (31.9-35.2)	34.6 \pm 0.8 (32.1-35.2)

The OSDI score (31.4 ± 22.4 vs. 17.5 ± 17.9), vision-related subscore (17.7 ± 14.6 vs. 10.5 ± 13.2), and discomfort-related subscore (14.3 ± 10.7 vs. 9.4 ± 10.5) were significantly higher in all KC patients and in all TKC subgroups, than in controls ($p \leq 0.034$). In the KC group, there was an increasing tendency in the OSDI scores and subscores along the increasing TKC stages, however these differences were not significant between the stages, except the KC3 and KC4 OSDI scores ($p=0.032$). (Németh et al, 2020a)

The average central OST was $34.2 \pm 0.6^\circ\text{C}$ in KC patients and $34.2 \pm 0.6^\circ\text{C}$ in controls ($p=0.56$). There was no significant difference in central ($34.2 \pm 0.6^\circ\text{C}$ vs. $34.2 \pm 0.7^\circ\text{C}$), nasal ($34.2 \pm 0.6^\circ\text{C}$ vs. $34.2 \pm 0.7^\circ\text{C}$), temporal ($34.2 \pm 0.6^\circ\text{C}$ vs. $34.2 \pm 0.6^\circ\text{C}$), and superior ($34.2 \pm 0.6^\circ\text{C}$ vs. $34.2 \pm 0.6^\circ\text{C}$) OST between the two groups ($p \geq 0.22$).

According to TKC, 24 eyes were classified as stage 1 (13.4%), 55 eyes as stage 2 (30.7%), 51 eyes as stage 3 (28.5%), and 24 eyes as stage 4 (13.4%). Patients with a TKC between two stages (e.g., TKC 0-1) were always classified as the more advanced stage. Using the Kruskal-Wallis test, OST between less and more advanced stages of KC did not differ; therefore, we did not perform a correlation analysis of the KC subgroups.

OSDI score poorly correlated with the SAI ($r=0.295$, $p < 0.001$) and fairly correlated with the SRI ($r=0.354$, $p < 0.001$), but did not correlate with OST at the corneal centre ($r=-0.012$) or other corneal or conjunctival regions ($r \geq -0.072$). OSDI also did not correlate with CCT in either group ($r=-0.270$). (Németh et al, 2020a)

For all participants, the correlation of the vision- and discomfort-related OSDI subscores with SAI, SRI, and OST at the corneal centre in different stages of KC is shown in **Table 4**. For all participants, vision- and discomfort-related OSDI subscores poorly to fairly correlated with SRI and SAI ($r > 0.174$, $p < 0.005$), but none of the subscores correlated with OST ($r < 0.001$). In some of the subgroups (control, KC1, and KC2), the subscores correlated poorly with SAI and SRI and the discomfort-related OSDI subscore poorly correlated with OST (**Table 4**). OST at all the examined regions also fairly correlated with patient age ($-0.177 \geq r \geq -0.310$) in the KC group and did not correlate with the control group ($-0.10 \geq r \geq -0.074$). OST at the corneal centre also did not correlate with the SAI ($r=-0.056$), SRI ($r=-0.086$), or CCT ($r=0.048$).

Table 4. Spearman correlation of vision- and discomfort-related Ocular Surface Disease Index (OSDI) subscores with surface characteristics at the corneal centre in different stages of keratoconus (KC) and controls (Németh et al, 2020a).

VR: vision-related, DR: discomfort-related, SAI: surface asymmetry index, SRI: surface regularity index, OST: ocular surface temperature

r values are given, with p-values shown in the case of significance.

	Central		
	SAI	SRI	OST
KC4 – VR OSDI	-0.29	-0.08	-0.18
KC3 – VR OSDI	-0.12	-0.05	-0.007
KC2 – VR OSDI	-0.07	0.26	0.03
	p=0.04		
KC1 – VR OSDI	0.33	0.02	0.35
Control – VR OSDI	0.22	0.32	-0.07
	p=0.03	p=0.002	
KC4 – DR OSDI	-0.18	0.24	-0.09
KC3 – DR OSDI	-0.27	-0.19	-0.04
KC2 – DR OSDI	-0.15	0.18	0.02
KC1 – DR OSDI	0.27	0.18	0.45
	p=0.02		
Control – DR OSDI	0.26	0.25	-0.01
	p=0.01	p=0.01	

4.2 Correlation between corneal endothelial cell density and central corneal temperature in normal and keratoconus eyes

ECD, hexagonality, the average coefficient of variation of corneal endothelial area (CV), CCT, OSDI score, and central and conjunctival OST are provided in **Table 5**. Corneal front and back surface radius of curvature (RmF/RmB) and corneal front and back surface area at a central 5 mm region (FSA/BSA) are shown at **Table 6**.

ECD (2498 ± 356 vs. $2638 \pm 294/\text{mm}^2$) and CCT (475 ± 50 vs. $529 \pm 35 \mu\text{m}$) were significantly lower ($p < 0.001$; $p < 0.001$) and CV (48.2 ± 18.3 vs. 47.3 ± 52.3) was significantly higher ($p = 0.001$) in KC patients than in healthy controls, but hexagonality (42.8 ± 22.7 vs. 38.9 ± 20.8) did not differ significantly between the two groups ($p = 0.69$).

The average central corneal OST was $34.2 \pm 0.6^\circ\text{C}$ in KC patients and $34.3 \pm 0.7^\circ\text{C}$ in controls and did not differ significantly ($p = 0.62$). Conjunctival OST ($34.4 \pm 1.0^\circ\text{C}$ vs. $34.6 \pm 0.8^\circ\text{C}$) also did not differ significantly between the two groups ($p = 0.21$). Using a Kruskal-Wallis test, we found no difference in OST between less and more advanced stages of KC; therefore, we did not proof for differences between TKC groups.

RmF (6.9 ± 0.8 vs. 7.7 ± 0.2) and RmB (5.6 ± 0.8 vs. 6.3 ± 0.2) were significantly lower ($p < 0.001$; $p < 0.001$), FSA (20.35 ± 0.26 vs. 20.17 ± 0.03) and BSA (20.84 ± 0.58 vs. 20.45 ± 0.08) were significantly higher in KC subjects ($p < 0.001$; $p < 0.001$), compared to controls.

ECD weakly positively correlated with central corneal OST ($r = 0.2$; $p < 0.05$) and did not correlate with conjunctival OST ($r = 0.043$). CV weakly negatively correlated with central corneal OST ($r = -0.212$; $p = 0.001$) and did not correlate with conjunctival OST ($r = -0.075$). Hexagonality did not correlate with the OST within the regions of interest ($r > 0.013$). CCT also did not correlate with central corneal OST ($r = 0.048$).

Figures 2-3. present the scatter plot analysis of central corneal OST and ECD; CV; hexagonality; CCT; OSDI; FSA and BSA in normal (TKC 0) and keratoconus eyes (TKC 1- TKC 4), with regression lines for TKC 0 and TKC 1-TKC 4 groups.

Table 5. Measurements in different topographic keratoconus classification (TKC) stages. Data are given as mean±SD (minimum-maximum). ECD, endothelial cell density; CV, coefficient of variation of corneal endothelial area; CCT, central corneal thickness; OSDI, Ocular Surface Disease Index; OST, ocular surface temperature (central: at corneal centre, conjunctival: 8 mm temporally from the corneal centre) (Németh et al, 2020b).

TKC	ECD (/mm ²)	Hexagonality (6A, %)	CV in %	CCT (µm)	OSDI	OST central (°C)	OST conjunctival (°C)
TKC 0 (n=92)	2638±294 (1813-3244)	38.9±20.8 (0-70)	47.3±52.3 (30-137)	529±35 (477-627)	19.3±18.3 (0-79.6)	34.3±0.7 (32.4-35.4)	34.6±0.8 (31.6-35.8)
TKC 1-TKC 4 (n=154)	2498±356 (1208-3245)	42.8±22.7 (0-100)	48.2±18.3 (23-126)	475±50 (366-563)	32.3±22.6 (0-88.9)	34.2±0.6 (32.4-35.4)	34.4±1.0 (30.8-36.3)
P value*	<0.001	0.69	0.001	<0.001	<0.001	0.62	0.21
TKC 1 (n=24)	2592±262 (2101-2988)	41.7±19.6 (0-65)	40.6±7.9 (30-58)	491±33 (408-538)	30.1±19.3 (4.2-60.4)	34.3±0.7 (32.4-35.4)	34.3±1.0 (31.9-35.9)
TKC 2 (n=55)	2528±350 (1595-3245)	49.1±20.9 (0-100)	47.6±16.4 (30-106)	471±44 (370-557)	31.7±25.2 (0-87.5)	34.2±0.6 (32.4-35.4)	34.5±0.9 (30.8-36.2)
TKC 3 (n=51)	2408±334 (1303-3047)	37.9±23.9 (0-100)	50.7±16.4 (30-115)	447±45 (366-527)	29.4±18.5 (4.2-88.9)	34.3±0.7 (32.4-35.4)	34.5±1.2 (31.1-36.3)
TKC 4 (n=24)	2380±397 (1208-3039)	35.3±24.1 (0-75)	59.1±27.7 (23-126)	449±62 (373-563)	41.6±25.9 (0-88.9)	34.2±0.6 (32.9-35.0)	34.5±0.9 (32.0-36.0)

*Difference between normal cornea (= TKC 0) and all eyes in TKC 1-TKC 4 groups. Patients with a TKC between two stages (e.g., 0-1) were always classified as the more advanced stage.

Table 6. Measurements in different topographic keratoconus classification (TKC) stages. Data are given as mean \pm SD (minimum-maximum). Corneal front and back surface radius of curvature (RmF/RmB) and corneal front and back surface area at a central 5 mm region (FSA/BSA) are shown (Németh et al, 2020b).

*Difference between normal cornea (= TKC 0) and all eyes in TKC 1-TKC 4 groups. Patients with a TKC between two stages (e.g., 0-1) were always classified as the more advanced stage

TKC	RmF (mm)	RmB (mm)	FSA (mm²)	BSA (mm²)
TKC 0 (n=92)	7.7 \pm 0.2 (7.1-8.5)	6.3 \pm 0.2 (5.6-7.2)	20.17 \pm 0.03 (20.07-20.29)	20.45 \pm 0.08 (20.25-20.72)
TKC 1-TKC 4 (n=154)	6.9 \pm 0.8 (4.3-8.4)	5.6 \pm 0.8 (3.2-7.4)	20.35 \pm 0.26 (20.09-21.69)	20.84 \pm 0.58 (20.23-24.13)
P value*	<0.001	<0.001	<0.001	<0.001
TKC 1 (n=24)	7.5 \pm 0.2 (7.2-8.0)	6.1 \pm 0.3 (5.6-6.8)	20.20 \pm 0.04 (20.14-20.27)	20.53 \pm 0.09 (20.33-20.72)
TKC 2 (n=55)	7.3 \pm 0.4 (6.5-8.4)	5.9 \pm 0.5 (4.9-7.4)	20.25 \pm 0.08 (20.09-20.43)	20.62 \pm 0.20 (20.23-21.07)
TKC 3 (n=51)	6.8 \pm 0.6 (5.4-8.4)	5.4 \pm 0.6 (4.0-6.9)	20.34 \pm 0.14 (20.09-20.81)	20.85 \pm 0.33 (20.32-22.05)
TKC 4 (n=24)	5.8 \pm 1.0 (4.3-7.7)	4.6 \pm 1.0 (3.2-6.9)	20.75 \pm 0.44 (20.19-21.69)	21.66 \pm 0.97 (20.32-24.13)

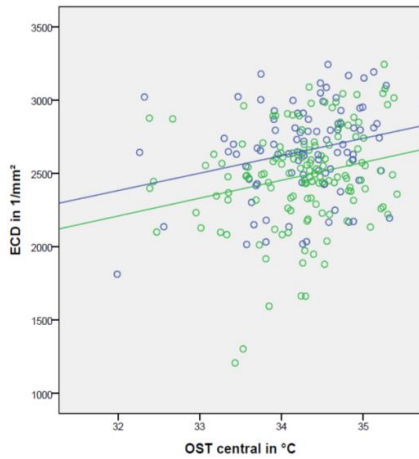
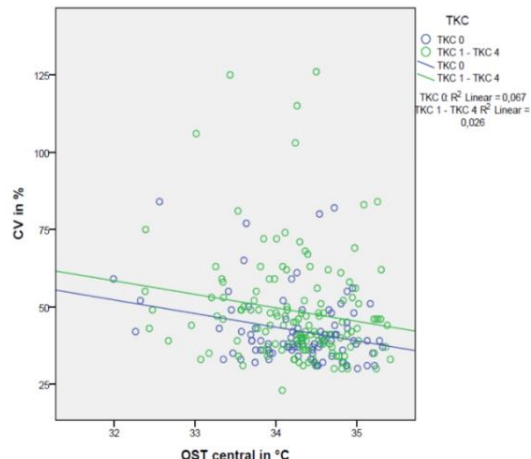
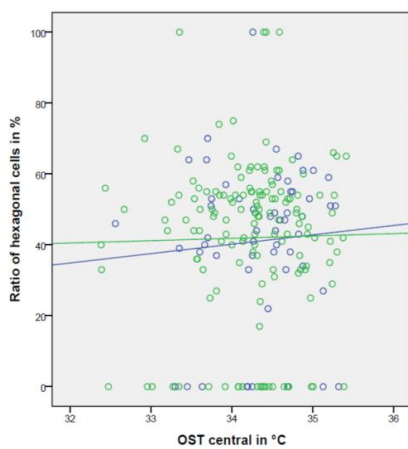
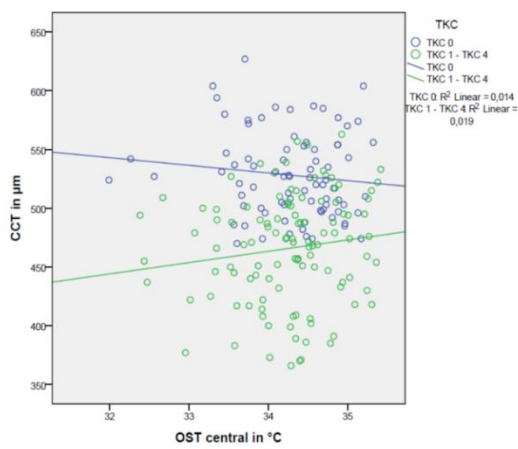
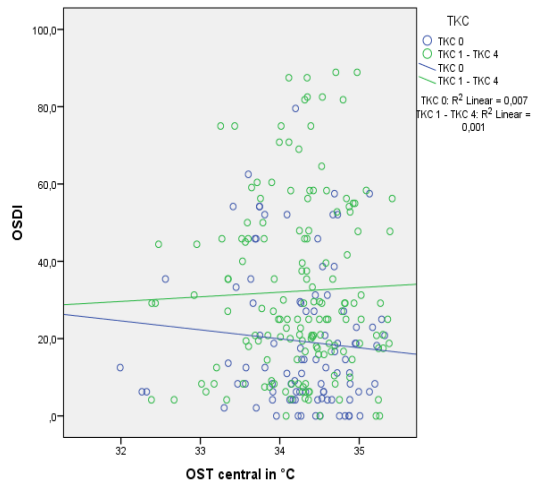
A**B****C****D****E**

Figure 2. Scatter plot of the central corneal ocular surface temperature (OST central) and endothelial cell density (ECD) (A)/coefficient of variation (CV) (B)/ ratio of hexagonal cells (C)/central corneal thickness (CCT)(D)/ Ocular Surface Disease Index (OSDI)(E) in normal corneas (TKC 0; n=92, blue circles and blue regression line) and keratoconus corneas (TKC 1-TKC 4; n=154, green circles and green regression line). Patients with a TKC between two stages (e.g., TKC 0-1) were always classified as the more advanced stage. R^2 refers to Spearman's coefficient of determination. (Németh et al, 2020b)

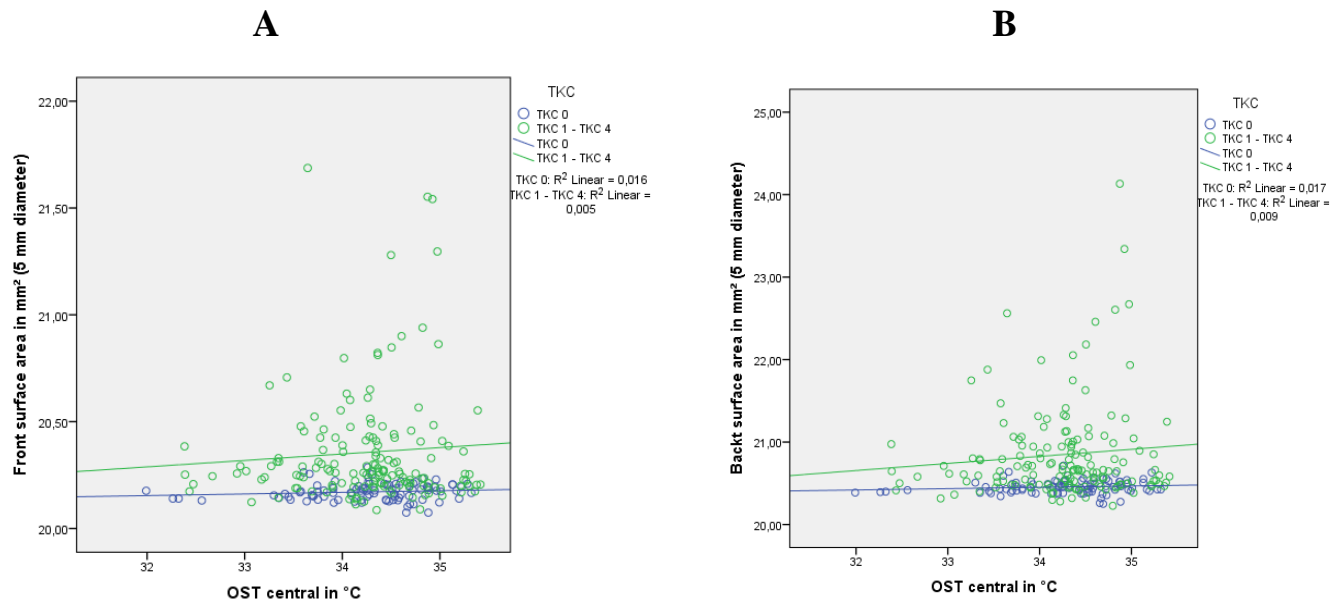


Figure 3. Scatter plot of the central corneal ocular surface temperature (OST central) and corneal front and back surface area (FSA/BSA) (A, B) in normal corneas (TKC 0; n=92, blue circles and blue regression line) and keratoconus corneas (TKC 1-TKC 4; n=154, green circles and green regression line). Patients with a TKC between two stages (e.g., TKC 0-1) were always classified as the more advanced stage. R^2 refers to Spearman's coefficient of determination. (Németh et al, 2020b)

RmF, RmB, FSA and BSA did not correlate with central corneal OST ($r=0.015$; $r=-0.024$; $r=0.045$; $r=0.064$). FSA and BSA did not correlate with ECD ($r=-0.186$; $r=-0.170$), hexagonality ($r=-0.131$; $r=-0.142$) and CV ($r=0.133$; $r=0.102$).

OST at all examined regions did not correlate with patient age ($r <-0.158$). ECD correlated weakly inversely with patient age ($r=-0.365$; $p <0.001$), whereas CV and hexagonality did not correlate with age ($r<0.104$).

4.3 Ocular Surface Disease Index, biomechanical properties and ocular thermography in a keratoglobus patient

We enrolled a 58 years-old male patient in our study. There was poliomyelitis, hearing disorder and alcohol abuse in the medical history.

In the present work, the right eye of the patient without previous ocular surgery have been examined. Keratoglobus was diagnosed by slitlamp examination on the right eye of the patient. There was a diffuse thinning of the cornea, from limbus to limbus. The OSDI Score was 32.14 (vision-related subscore: 16.67, discomfort-related subscore: 15.625), referring to a moderate ocular surface disease.

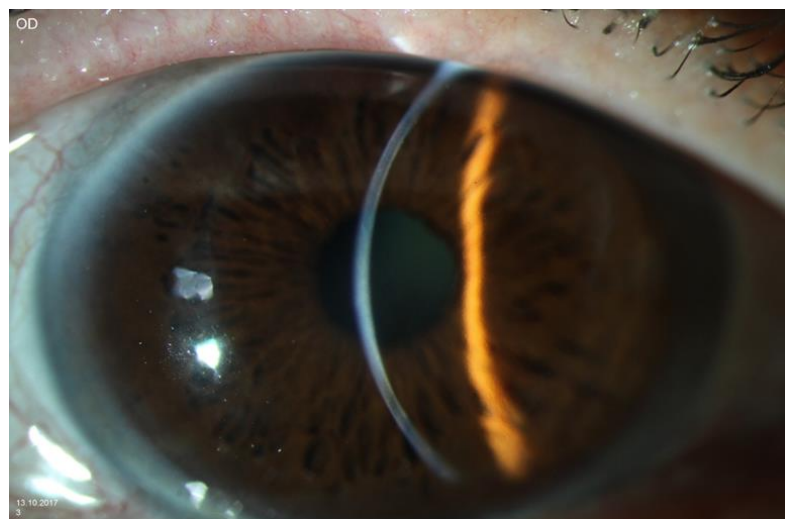


Figure 4. Diffuse thinning of the cornea from limbus to limbus at slitlamp examination (Németh et al, 2020c).

The left eye of the patient underwent cataract surgery in 2017, which ended up in corneal hydrops with a break in the Descemet membrane, and SF6 gas insufflation into the anterior chamber. However, corneal decompensation persisted and therefore, in October 2017, the patient underwent penetrating keratoplasty of the left eye. At our examination, best corrected visual acuity was on the right side 0.1 and on the left side 0.7 (decimal).

Figures 5 and 6 show results of the topo- and tomographic measurements. Corneal topography displays an increased corneal steepening at the 3/5/7 mm zones. The topographic cylinder (CYL) and the SAI increased, the SRI and the Potential Visual Acuity (PVA) were borderline compared to the normal database (**Figure 5**). Corneal tomography shows approximetry 20 diopters of corneal astigmatism and pathological ISV, IVA, IHD and Topographic Keratoconus Classification (TKC) (**Figure 6**).

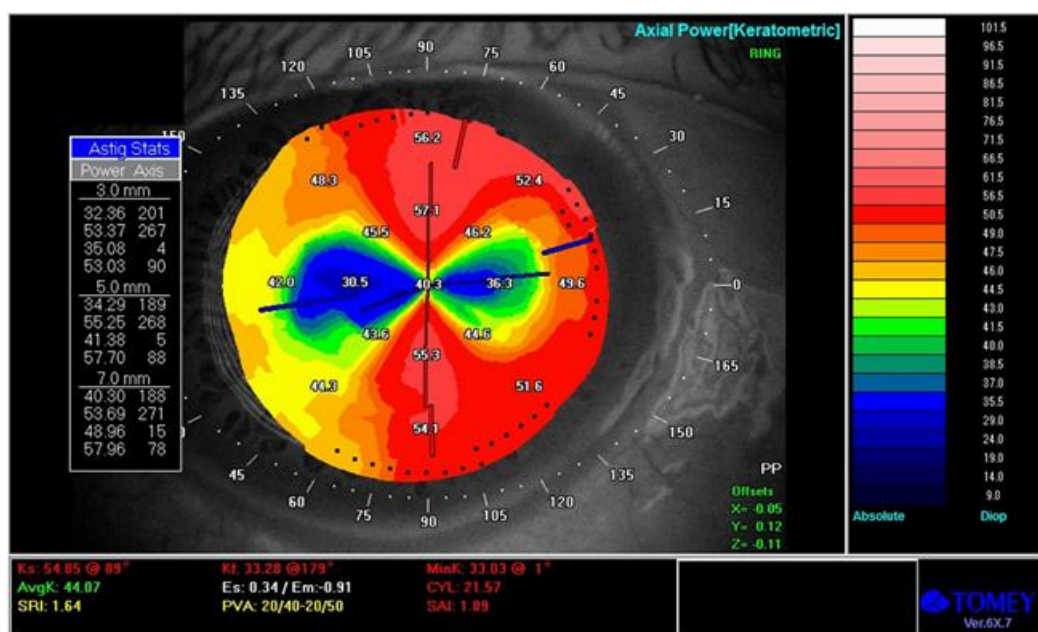


Figure 5. Corneal topography using the TMS-5 (Tomey, Erlangen-Tennenhole, Germany) in keratoglobus. The topographic cylinder (CYL) and the Surface Assimmetry Index (SAI) increased pathologically, the Surface Regularity Index (SRI) and the Potential Visual Acuity (PVA) measurements indicate borderline values (Németh et al, 2020c).

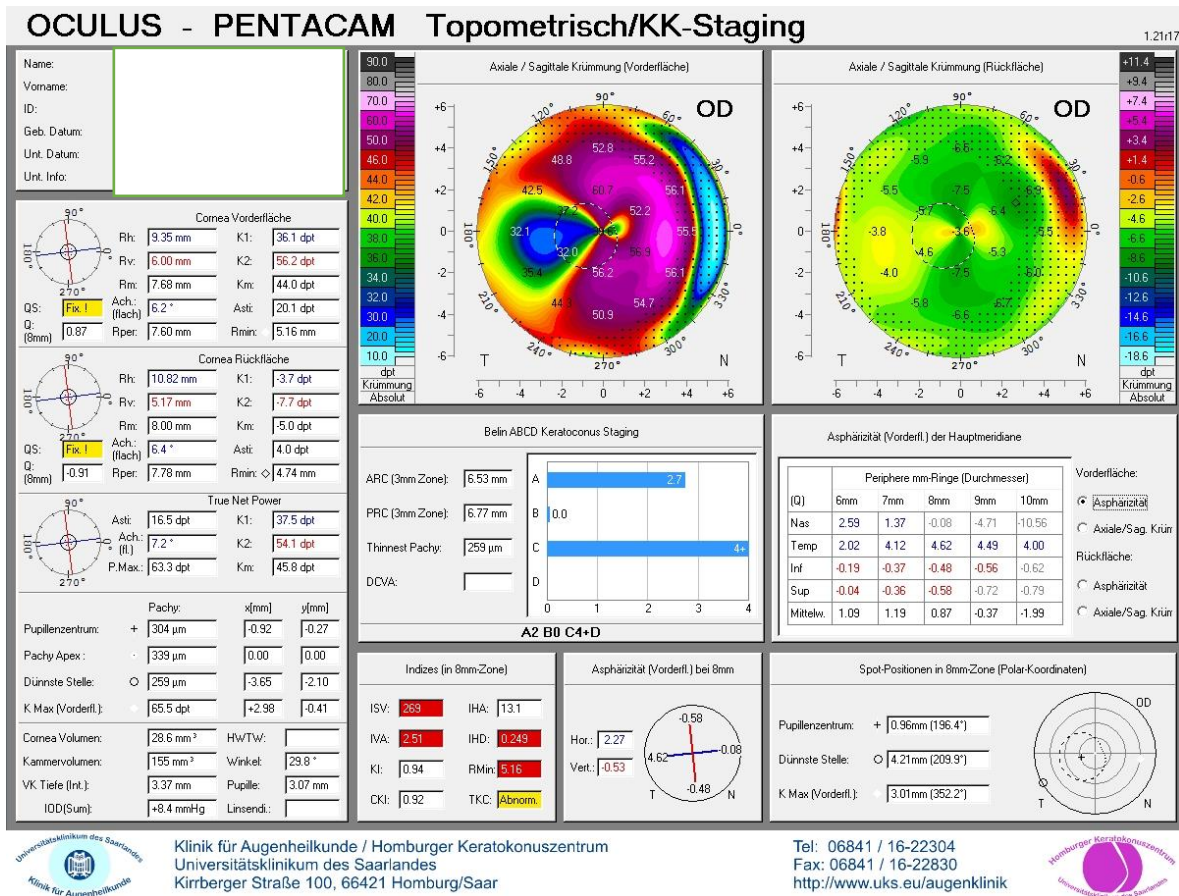


Figure 6. Corneal tomography measured by the Pentacam HR (Oculus, Wetzlar, Germany) in keratoglobus. The keratometric values, the Index of Surface Variance (ISV), the Index of Surface Asymmetry (IVA), the Index of Height Decentration (IHD) and the „Topographic Keratoconus Classification (TKC)” were abnormal (Németh et al, 2020c).

With the Corvis ST, the Stiffness parameter at applanation 1 (SPA1) was 29.3, the integrated radius (IR) 14.2 and the deformation appilitude ratio (DA ration) 3.6, but the Ambrósio's relational thickness Horizontal (ArtH) value could not be determined (**Figure 7**).

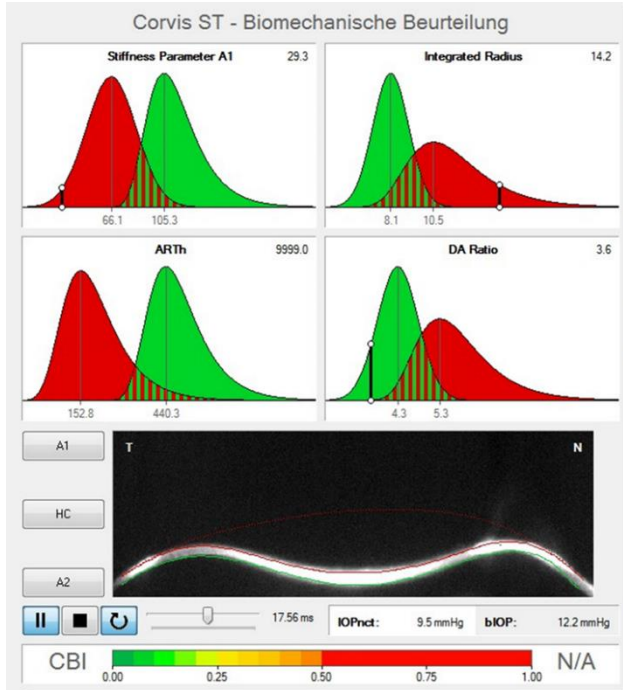
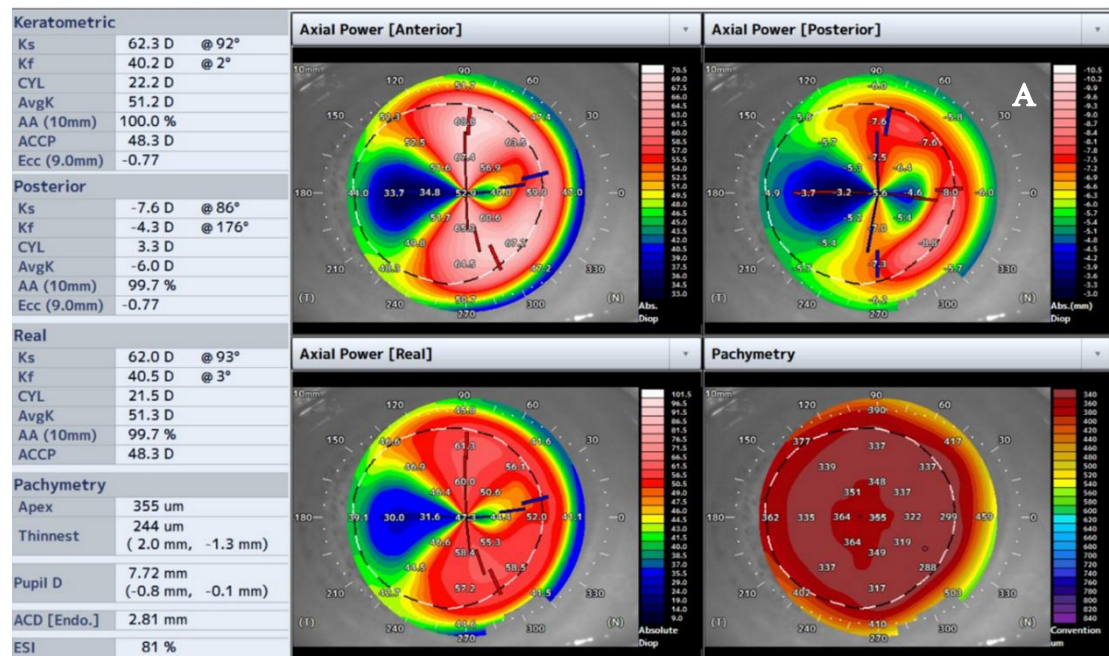


Figure 7. Screenshot of a CorVis ST measurement, performed by the dynamic corneal response modul of the machine. The area under the red curve corresponds to the parameters of the keratoconus patients, the area under the green curve corresponds to the normal database (Németh et al, 2020c).

Stiffness parameter at applanation 1 (SPA1) was 29.3, the integrated radius (IR) 14.2 and the deformation appitude ratio (DA ration) 3.6, but the Ambrósio's relational thickness Horizontal (ArtH) value could not be determined.

With the Casia 2 anterior segment optical coherence tomography, the diffuse corneal thinning from limbus to limbus is well demonstrated (**Figure 8**).



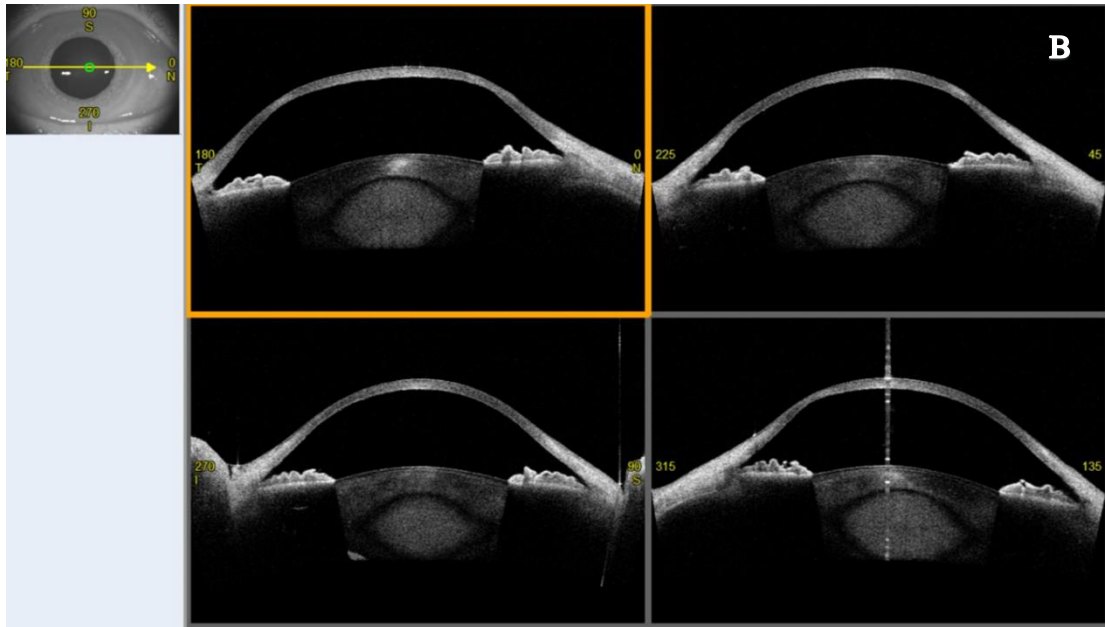


Figure 8. Casia-2 anterior segment optical coherence tomography (AS-OCT) in a keratoglobus patient. Anterior, posterior and real axial refractive power of the cornea and the a pachymetric map (A) prove the diagnosis of keratoglobus. Analysing the anterior segment cross-sectionally, the diffuse thinning of the cornea is well demonstrated (B) (Németh et al, 2020c).

The ocular surface temperature was measured after normal blinking. The patient was asked to keep his eyes close for 5 seconds, than he opened them and the measurement was started, immediately after eye opening. During 10 seconds of sustained eye opening, we measured the ocular temperature. The software automatically displayed a graph (**Figure 9.**) of the OST changes.

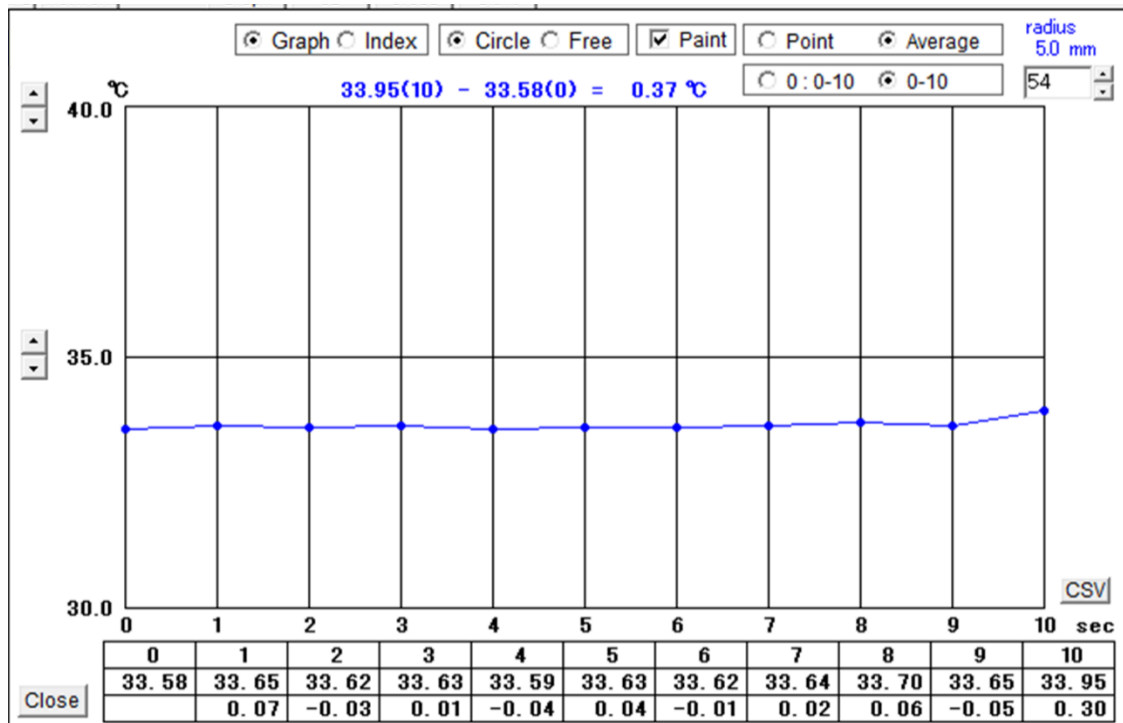


Figure 9. Ocular surface temperature in a keratoglobus patient, measured by the TG-1000 thermographer. Ocular surface temperature is displayed in the central 5 mm corneal zone, during 10 seconds of eye opening, after blinking (Németh et al, 2020c).

The average minimal ocular surface temperature was 33.58 °C and the average maximal ocular surface temperature was 33.95 °C.

5. Discussion

5.1 Ocular Surface Disease Index and ocular thermography in keratoconus patients

The most conspicuous finding of our study is that OST does not differ between KC patients and controls, though the OSDI score was significantly higher in KC patients than in controls. In addition, OST at the corneal centre did not correlate with SAI, SRI, TKC ($p \geq 0.18$), CCT, PCP, or PCA ($p \geq 0.06$). OSDI score and vision- and discomfort-related OSDI subscores poorly to fairly correlated with the SAI and SRI, but did not correlate with central corneal OST (Németh et al, 2020a).

The aetiology of KC remains unclear. However, several authors have discussed a potential inflammatory cofactor (Lema et al, 2009; Kolozsvári et al, 2014; Pásztor et al, 2016). Allergic conjunctivitis and dry eye syndrome are common among KC patients (Weed et al, 2008; De Paiva et al, 2003). In patients with dry eye, the OST is increased, and OST decreases quicker during sustained eye opening than in healthy adults (Klammann et al, 2013; Kawali 2013, Kamao et al 2011). Moussa et al. (Moussa et al, 2013) could not find any diurnal changes in the OST of healthy adults. Morgan et al. (Morgan et al, 1995) also found an increase in the OST throughout the day, especially in dry eyes. These findings suggest that diurnal changes in OST indicate ocular surface abnormalities or corneal pathology. Analysing the diurnal changes in the OST of KC patients was not the aim of the present study, but it could be interesting to assess the diurnal variations in OST in KC patients in the future (Németh et al, 2020a).

Hara et al. found a significant correlation between the conjunctival surface temperature and the severity of conjunctival allergic disease, and OST was a useful measure to determine the effectiveness of antiallergy agents (Hara et al, 2014). The increase in OSDI score in KC patients may reflect dry eye disease, or could be related to the poor visual outcomes in KC patients. With an increase in both the vision- and discomfort-related OSDI subscores in KC, we could determine that both ocular surface disease and deteriorated visual acuity contribute to the increased OSDI score. However, this is not

mirrored by an increase in the OST (Németh et al, 2020a). Data on conjunctival allergic disease was not collected in the present study.

Corneal innervation may also play a decisive role in OST. The cornea is densely innervated by the fibres of the ophthalmic branch of the trigeminus nerve, known as ciliary nerves (Muller et al, 1996). Corneal nerves are important for corneal homeostasis due to their protective functions, their role in wound healing, and in regulating corneal sensation (Guthoff et al, 2005; Oliveira-Soto et al, 2001). Epithelial dendritic cells (Langerhans cells) are inflammatory, antigen-presenting corneal cells responsible for immune surveillance. These cells are distributed from the basal epithelial corneal layer to the subbasal nerve plexus (Zhivov et al, 2005). Mature Langerhans cell morphology is frequently seen in the periphery of the cornea, whereas immature cells are seen centrally (Zhivov et al, 2007).

The subbasal nerve plexus and the epithelial dendritic cell density have been examined in different subtypes of dry eye disease. Tepelus et al. (Tepelus et al, 2017) found a reduction in the subbasal nerve plexus and an increase in inflammatory dendritic cell density in Sjögren and non-Sjögren dry eye subgroups (Ucakhan et al 2006). Many studies have demonstrated abnormal corneal nerve morphology and branching patterns, reduced nerve density, increased tortuosity, and thickening in KC (Ucakhan et al, 2006; Bitirgen et al, 2015). Mandathara et al. found mature Langerhans cells at the centre of the cornea, which also supports an inflammatory origin of KC (Mandathara et al, 2018). To the best of our knowledge, the relationship between changes in the subbasal nerve plexus and Langerhans cell density and OST has not yet been analysed.

The literature offers controversial information on the effect of corneal thickness on OST. Morgan reported a significant decrease in OST with increasing corneal thickness (Morgan 1994). In contrast, Alio et al. (Alió et al, 1982) and Efron et al. (Efron et al, 1989) found a progressive increase in OST from the corneal centre to the periphery. Purslow et al. (Purslow et al 2007) found a weak negative correlation between corneal thickness and OST using the Thermo Tracer 7210MX. Pattmöller et al. (Pattmöller et al, 2015) could not verify a correlation between local corneal thickness and local OST at any point on the corneal surface in healthy adults. If OST is affected by anterior chamber depth is also controversial (Alió et al, 1982; Efron et al, 1989; Pattmöller et al, 2015). In the present

study, we could not determine a correlation between corneal thickness and OST in KC patients or controls (Németh et al, 2020a).

In summary, we found a significantly increased OSDI score in KC patients compared to an age-matched control group. However, this was not accompanied by an increase in the OST at any stage of KC. We could not clarify whether the reduced corneal thickness in KC patients may have a “corneal-cooling effect”. Our study also shows that both vision- and discomfort-related symptoms of KC have to be managed in parallel in ophthalmologic practice, but the necessity of anti-inflammatory treatment cannot be verified through ocular thermography.

5.2 Correlation between corneal endothelial cell density and central corneal temperature in normal and keratoconus eyes

The most conspicuous finding of our study is that OST at the corneal centre correlates weakly positively with ECD and weakly negatively with CV. Interestingly, we demonstrated these weak correlations in both keratoconus and healthy eyes. Nevertheless, no correlation between RmF, RmB, FSA, BSA and central corneal OST could be verified in our present study. These results rather show that ECD has a special role in regulation of OST, without an influence of the corneal front/back surface curvature and area (Németh et al, 2020b).

We hypothesized, that an increase of the corneal back surface area results in ECD decrease and parallelly, an increase of the corneal front surface area results in OST decrease due to increased heat dissipation in keratoconus eyes. Although there was a significantly lower ECD (and higher CV) in keratoconus eyes than in controls, a significant difference in OST could not be shown between the patient groups, so this fact contradicted our hypothesis (Németh et al, 2020b)..

Kitazawa et al. (Kitazawa et al, 2018) described the ratio of the front and back corneal surface area in keratoconus smaller than in normal eyes. Therefore, a significant difference in ECD, without a significant difference in OST between KC and normal eyes (as corneal front surface increases less than corneal back surface in KC and there is less heat dissipation), could probably be explained. Nevertheless, that RmF, RmB also did not

correlate with OST in the examined KC and control subjects, contradicts again our hypothesis. Therefore, we rather assume, that ECD has a mild role in OST regulation, without an influence of the corneal front/back surface curvature and area, which should be further explored in the future.

The corneal epithelial and endothelial barrier plays a major role in the maintenance of corneal transparency (Mergler et al, 2007). If corneal endothelium is compromised, the cornea becomes thicker, oedematous, and loses its transparency (Edelhauser et al, 1982). Acting as a permeability barrier, the endothelial monolayer restricts the flow of aqueous humour and solutes into the hydrophilic stroma (Mergler et al, 2007). In addition, there is endothelial active ion transport (Huff et al, 1981) from the stroma to the aqueous humour. This mechanism corresponds to a combined leaky barrier and fluid pump (Mergler et al, 2007). The maintenance of corneal thickness and transparency is based on a balance of fluid inflow leaking into the stroma and outflow being actively pumped out from the stroma by the endothelium (Bourne 1998). As we have proven ECD to be weakly correlated with central corneal temperature, it would be important to analyse patients with endothelial pathologies such as bullous keratopathy or Fuchs' dystrophy. OST may be capable to detect early endothelial dysfunction in such cases.

Long-standing corneal oedema also predisposes individuals to complications, such as corneal vascularisation, infection, and scarring (Luchs et al, 1997). Elevated cytokine levels have been reported in the aqueous humour of eyes with bullous keratopathy and low endothelial density, which reflects inflammation in this condition. Elevated cytokine levels have also been described in tears of keratoconus patients, but as OST positively correlated with ECD in keratoconus patients of our present study, this contradicts an inflammatory hypothesis (Yamaguchi et al 2016). If elevated cytokine levels are related to an OST increase, also requires further analysis.

Endothelial cell morphology reflects the quantitative corneal properties and provides a qualitative description of the functional status, in regards to variation in the cell area and shape. The quality of corneal endothelium may not be assessed by cell density measurements alone, but by quantification of the CV, the percentage of hexagonal cells, and the CCT (Costagliola et al, 2013). Although our KC patients had significantly lower ECD and higher CV than controls, we could not find a difference in the hexagonality of the cells between both groups. Nevertheless, plenty of other factors such as dry eye

syndrome or type 2 diabetes mellitus may decrease ECD/function and change hexagonality (El-Agamy et al, 2017; Kheirkhah et al, 2015). Similar to our present study, according to Goebels et al. (Goebels et al, 2018) in KC, corneal thickness and ECD are significantly decreased and endothelial CV significantly increased with the progression of KC severity (Németh et al, 2020b).

During aging, corneal ECD decreases by 0.3% to 1% per year (Niederer et al, 2007). This phenomenon is also observed in our data set, as ECD correlated with patient age.

Pattmöller et al. (Pattmöller et al, 2015) analysed the correlation of OST and ECD at the corneal centre in 61 Caucasian healthy adults (mean age 24.9 ± 6.7), also using the TG-1000 thermographer. They concluded that in young healthy adults, the average ocular surface temperature does not correlate with ECD, which contradicts our present study. However, for their examination, all dry eye subjects have been excluded and patient age was 10 years lower compared to our present study population. In addition, air humidity was different during their examination ($41.83 \pm 4.19\%$ vs. $32.4 \pm 6.7\%$). Changes in environmental factors may have a significant impact on OST measurements. Additional drawback of both studies is that body temperature has not been measured immediately before OST measurements.

Schroeter et al. (Schroeter et al, 2008, 2015) analysed the impact of temporary hypo- and hyperthermia on corneal endothelial cell survival during organ culture preservation. The exposure of organ-cultured porcine corneas to 4°C for 12 hours and 21°C for 48 hours did not compromise the endothelial cell density of donor corneas in a clinically relevant manner (Schroeter et al, 2008). Exposure of the porcine corneas to 40°C or 42°C for 12 h also did not induce endothelial cell loss (Schroeter et al, 2015). Nevertheless, exposure to 44°C and 50°C led to total necrosis of the endothelial cell layer (Schroeter et al 2015). These findings show that temperature changes of the ocular surface below 40°C may not have an impact on the endothelial cell layer. This is especially important concerning corneal organ cultures and corneal storage temperature. Nevertheless, measurement series with a longer exposure time should further strengthen this hypothesis as in our in vivo study, ECD weakly correlated with the ocular surface temperature.

OST was measured under different ophthalmological conditions. Tai-Yuan Su et al. (Su et al, 2017) found that the eyelid margin temperature is higher in cases of Meibomian gland dysfunction than in healthy controls. Furthermore, according to Morgan et al.

(Morgan et al, 1995), the mean OST is larger in dry eye than controls, and larger variation in temperature was measured across the ocular surface in the dry eye group. The OST is also higher when a corneal ulcer is present (Klamman et al, 2013) and in corneal immunological transplant rejection (Sniegowski et al 2018), compared to normal eyes. The OST has been investigated to analyse bleb function after glaucoma surgery (Kawasaki et al, 2009), after corneal refractive surgery (Betney et al 1997), following cataract surgery (Belkin et al, 2017) and in ocular blood flow evaluation (Konieczka et al, 2018). However, to the best of our knowledge, this is the first study to analyse the relationship between OST and corneal ECD in a corneal pathology (Németh et al, 2020b). It would be interesting to analyse in future studies whether, under pathological conditions (e.g., blepharitis, dry eye, corneal ulcer, corneal transplant rejection, glaucoma, following corneal refractive or cataract surgery) (Klamann et al, 2013; Morgan et al, 1995; Sniegowski et al, 2018; Kawasaki et al, 2009; Betney et al, 1997; Belkin et al, 2017; Konieczka et al, 2018), ECD also has an impact on OST.

In summary, endothelial cell density seems to have a mild impact on central ocular surface temperature in keratoconus and normal subjects. This effect is not correlated to corneal front or back surface area or curvature. The exact reason for this phenomenon remains unclear.

5.3 Ocular Surface Disease Index, biomechanical properties and ocular thermography in a keratoglobus patient

Keratoglobus is characterized by diffuse corneal thinning with progressive myopia and irregular astigmatism. The topographic features of keratoglobus were first described by Karabatsas et al in 1996 (Karabatsas et al, 1996). According to his description, keratoglobus is the progressive form of other ectatic corneal disorders, with an increase of the refractive power also closed to the limbus (Karabatsas et al, 1996). Therefore, they suggested, that keratoglobus was an advanced stage of pellucide marginale degeneration (Karabatsas et al, 1996). In addition, similar to keratoconus, ruptures in the Bowman layer and the Descemet's membrane may also be present in keratoglobus. Due to these common histological features, both ectatic corneal diseases (keratoconus and keratoglobus) may also be similar (Rabinowitz 1998).

In our work, we first described biomechanical properties of a keratoglobus eye (Németh et al, 2020c). The CorVis ST is an ultra high-speed Scheimpflug camera, which is able to determine several corneal deformation parameters such as applanation time, applanation length, applanation velocity, deformation and deflection amplitude, peak distance, stiffness parameter-applanation time 1, Corvis Biomechanical index. Changes of the corneal biomechanical properties are described to be pathognomonic in early stages of keratoconus. The Biomechanical Index of the Corvis (CBI) (> 0.50) is able to identify keratoconus (98.8%), with 98.4 % sensitivity and 100 % specificity (Vinciguerra et al, 2016). Tomography and the biomechanical index (> 0.79) together could differentiate ectatic disorders with 100 % specificity and sensitivity (Ambrosió et al, 2017). In addition, decrease of the corneal biomechanical properties correlates with the stage of keratoconus (Johnson et al, 2015). The SP-A1 is a parameter reflecting bending stiffness of the cornea as defined by force/replacement. SP-A1 value is lower in thinner corneas (Vinciguerra et al, 2016). Also in our keratoglobus patient, the SP-A1 decreased. The integrated radius value was described to be lower in keratoconus, as we measured for the keratoglobus eye. The Ambrósio's relational thickness Horizontal value (ArH) was not detectable and the DA ratio was within the normal range for our keratoglobus eye. In contrast to the examined keratoglobus eye, DA value in keratoconus was described to be higher than in normal eyes. DA ratio describes the ratio between deformation amplitude at the corneal apex and the average deformation amplitude in the nasal and temporal zone 1 mm and 2 mm from the corneal centre (Chan et al, 2018). The greater the difference between the centre and defined paracentral regions, the less resistant is the cornea to deformation (Chan et al, 2018). As keratoglobus is characterised by a diffuse corneal thinning from limbus to limbus, it may be understandable that this difference did not exist in our keratoglobus eye and therefore, was not displayed in the DA ratio. According to these findings, using the DA value, we can distinguish between keratoglobus and keratoconus patients. Nevertheless, we can not generalize these data, as first studies with higher number of subjects with keratoglobus should be performed, to get general conclusions before conducting studies in a bigger population of keratoglobus patients (Németh et al, 2020c).

Results of the OSDI questionarie suggest moderate ocular surface disease in our keratoglobus patient. We may also analyse vision and discomfort related OSDI subscores.

In our study, the OSDI questionnarie indicate 52 % vision related and 48 % discomfort related symptoms in our keratoglobus patient. Nevertheless, we may not forget, that the OSDI questionarrie analyses symptoms of both eyes of a patient, a specific information on the eye without previous ocular surgery could not be gained. This also needs detailed analysis in the future to get a better insight into dry eye symptoms of keratoglobus patients (Németh et al, 2020c).

The average minimal and maximal ocular surface temperature at the corneal centre was 33.5 and 33.9 °C in keratoglobus. In case of healthy adults, the average ocular surface temperature is between 32.5-36.5 °C. Our value is within the lower part of this range, despite the moderate ocular surface disease, reflected through OSDI. This phenomenon could be explained by the higher vision related subscore of the OSDI, in our patient. In case of dry eye syndrome, the ocular surface temperture is higher than in healthy adults and OST decreases faster during sustained eye opening than in normal patients (Kawali et al, 2013). According to our earlier study, there is no significant difference in OST of keratoconus and normal subjects. Meanwhile, OSDI score is significantly higher in the keratoconus group. For keratoconus, this could be explained by the decreased visual function and increased ocular discomfort (Németh et al, 2020a). In the literature it is still not clear, if the corneal thickness could have an affect on the ocular surface temperature. Morgan et al (Morgan et al, 1995) measured significantly lower OST with higher corneal thickness. But on the other hand, Alió et al (Alió et al, 1982) and Efron et al (Efron et al, 1989) found increasing OST from the centre of the cornea to the limbus. Pattmöller et al (Pattmöller et al, 2015) could not find significant correlation between the corneal thickness and the OST. In keratoglobus, the relationship between corneal thickness and OST could not be verified analysing our single patient (Németh et al, 2020c).

In summary, despite slightly increased OSDI, ocular surface temperature was in the lower range of the normal range in the keratoglobus eye. Stiffness Parameter and DA ratio were decreased and Integrated Radius was increased in the keratoglobus eye, compared to the standard database of the Corvis ST. Our findings may help to differentiate keratoglobus from pellucid marginal degeneration/keratotorus and classical keratoconus in a clinical setting. However, studies on a larger group of patients are warranted to draw meaningful conclusions.

6. Conclusions

In our study, we aimed to analyse using ocular surface thermography, whether keratoconus and keratoglobus are in part inflammatory corneal diseases.

We found a significantly increased OSDI score in KC patients compared to an age-matched control group. However, this was not accompanied by an increase in the OST at any stage of KC. The increase in OSDI score in KC patients may reflect dry eye disease, or could be related to the poor visual outcome. With an increase in both the vision- and discomfort-related OSDI subscores in KC, we could determine that both ocular surface disease and deteriorated visual acuity contribute to the increased OSDI score. We could not clarify whether the reduced corneal thickness in KC patients may have a “corneal-cooling effect” (Németh et al, 2020a).

Our study also shows that both vision- and discomfort-related symptoms of KC have to be managed in parallel in ophthalmologic practice, but the necessity of anti-inflammatory treatment cannot be verified through ocular thermography.

ECD tends to correlate positively and CV negatively with central corneal temperature in both KC and healthy eyes. In case of higher ECD, the central corneal temperature seems to be higher, and in case of higher CV it seems to be lower. The reason for this phenomenon remains unclear (Németh et al, 2020b).

Despite slightly increased OSDI, ocular surface temperature was in the lower range of the normal range in the keratoglobus eye. Stiffness Parameter and DA ratio were decreased and Integrated Radius was increased in the keratoglobus eye, compared to the standard database of the Corvis ST. Our findings may help to differentiate keratoglobus from pellucid marginal degeneration/keratotorus and classical keratoconus in a clinical setting. However, studies on a larger group of patients are warranted to draw meaningful conclusions (Németh et al, 2020c).

Using ocular thermography, the inflammatory origin of keratoconus and keratoglobus could not be verified in our studies.

7. Summary

Several studies discuss the potential inflammatory origin of ectatic corneal diseases. Ocular thermography may be a helpful method to differentiate between diseases with and without an inflammatory origin. In addition, in corneal ectatic diseases, the concomitant eye rubbing, atopy, dry eye disease could also influence ocular surface termographic measurements. In our studies, we aimed to analyse using ocular surface thermography, whether keratoconus and keratoglobus are in part inflammatory corneal diseases.

We found an increased OSDI score in KC patients compared to an age-matched control group. However, this was not accompanied by an increase of the OST at any stage of KC. The OST in keratoconus did not differ from the OST of normal healthy adults, despite the difference of the OSDI between both groups. We could not clarify whether the reduced corneal thickness in KC patients may have a “corneal-cooling effect”. Our study also shows that both vision- and discomfort-related symptoms of KC have to be managed in parallel in ophthalmologic practice, but the necessity of anti-inflammatory treatment cannot be verified through ocular thermography (Németh et al, 2020a).

ECD tended to correlate positively and CV negatively with central corneal temperature in both KC and healthy eyes. In case of higher ECD, the central corneal temperature was higher, and in case of higher CV it seemed to be lower. Nevertheless, RmF and RmB did not correlate with OST in the examined KC and control subjects. The reason for this phenomenon remains unclear. Our research group was the first to describe the potential correlation of ECD with ocular surface temperature in keratoconus and normal eyes (Németh et al, 2020b).

Despite slightly increased OSDI, ocular surface temperature was in the lower range of the normal range in the keratoglobus eye. With other words the increased OSDI score was not mirrored by an increased OST in keratoglobus. Stiffness Parameter and DA ratio were decreased and Integrated Radius was increased in the keratoglobus eye. Our findings may help to differentiate keratoglobus from pellucid marginal degeneration/keratotorus and classical keratoconus in a clinical setting (Németh et al, 2020c).

In summary, using ocular thermography, the inflammatory origin of keratoconus and keratoglobus could not be verified in our studies.

8. References

1. Alió J, Padron M. (1982) Influence of age on the temperature of the anterior segment of the eye. Measurements by infrared thermometry. *Ophthalmic Res*, 14:153-159.
2. Ambrósio R Jr, Correia FF, Lopes B, Salomão MQ, Luz A, Dawson DG, Elsheikh A, Vinciguerra R, Vinciguerra P, Roberts CJ. (2017) Corneal Biomechanics in Ectatic Diseases: Refractive Surgery Implications. *Open Ophthalmol J*. 31;11: 176-193.
3. Baillif S, Garweg JG, Grange JD, Burillon C, Kodjikian L. (2005) Keratoglobus: review of the literature. *J Fr Ophthalmol*, 2810:1145–1149.
4. Belkin A, Abulafia A, Michaeli A, Ofir S, Assia EI. Wound temperature profiles of coaxial mini-incision versus sleeveless microincision phacoemulsification. (2017) *Clin Exp Ophthalmol*, 45: 247– 253.
5. Bereau J, Fabre EJ, Hecquet C, Pouliquen Y, Lorans G. (1993) Modification of prostaglandin E2 and collagen synthesis in keratoconus fibroblasts associated with an increase of interleukin-1 alpha receptor number. *CR Acad Sci III*, 316:425–430.
6. Betney S, Morgan PB, Doyle SJ, Efron N. (1997) Corneal temperature changes during photorefractive keratectomy. *Cornea*, 16:158–161.
7. Bitirgen G, Ozkagnici A, Bozkurt B, Malik RA. (2015) In vivo corneal confocal microscopic analysis in patients with keratoconus. *Int J Ophthalmol*, 18; 8:534-539.
8. Bourne WM. Clinical estimation of corneal endothelial pump function. (1998) *Trans Am Ophthalmol Soc*, 96: 229–239.
9. Cameron JA. (1993) Corneal abnormalities in Ehlers-Danlos syndrome type VI. *Cornea*, 12:54–59.
10. Cameron JA. (1993) Keratoglobus. *Cornea*, 122:124–130.
11. Chan TC, Wang YM, Yu M, Jhanji V. (2018) Comparison of corneal dynamic parameters and tomographic measurements using Scheimpflug imaging in keratoconus. *Br J Ophthalmol*, 102:42–47.

12. Chang HY, Chodosh J. (2013) The genetics of keratoconus. *Semin Ophthalmol*, 28: 275–280.
13. Costagliola C, Romano V, Forbice E, Angi M, Pascotto A, Boccia T, Semeraro F. (2013) Corneal oedema and its medical treatment. *Clin Exp Optom*, 96:529–535.
14. De Paiva CS, Harris LD, Pflugfelder SC. (2003) Keratoconus-like topographic changes in keratoconjunctivitis sicca. *Cornea*, 22:22–24.
15. Dienes L, Kiss HJ, Perényi K, Nagy ZZ, Acosta MC, Gallar J, Kovács I. (2015) Corneal Sensitivity and Dry Eye Symptoms in Patients with Keratoconus. *PLoS One*, 10:e 0141621.
16. Dogru M, Karakaya H, Ozçetin H, Ertürk H, Yücel A, Ozmen A, Baykara M, Tsubota K. (2013). Tear function and ocular surface changes in keratoconus. *Ophthalmology*, 110:1110–1118.
17. Edelhauser HF, Hyndiuk RA, Zeeb A, Schultz RO. (1982) Corneal edema and the intraocular use of epinephrine. *Am J Ophthalmol*, 93:327–333.
18. Efron N, Young G, Brenna NA. (1989) Ocular surface temperature. *Curr Eye Res*, 8:901-906.
19. Eghrari AO, Riazuddin SA, Gottsch JD. (2015) Overview of the cornea: structure, function, and development. *Prog Mol Biol Transl Sci*, 134:7-23.
20. El-Agamy A, Alsubaie S. (2017) Corneal endothelium and central corneal thickness changes in type 2 diabetes mellitus. *Clin Ophthalmol*, 11: 481–486.
21. Elbaz U, Mireskandari K, Tehrani N, Shen C, Khan MS, Williams S, Ali A. (2017) Corneal endothelial cell density in children: normative data from birth to 5 years old. *Am J Ophthalmol*, 173:134-138.
22. Feizi S. (2018) Corneal endothelial cell dysfunction: etiologies and management. *Ther Adv Ophthalmol* 2018; 10: 2515841418815802.
23. Freeman RD, Fatt I. (1973) Environmental influences on ocular temperature. *Invest Ophthalmol Vis Sci*, 12:596–602.
24. Fukuchi T, Yue BY, Sugar J, Lam S. (1994) Lysosomal enzyme activities in conjunctival tissues of patients with keratoconus. *Arch Ophthalmol*, 112: 1368–1374.

25. Garcia-Ferrer FJ, Akpek EK, Amescua G, Farid M, Lin A, Rhee MK, Varu DM, Musch DC, Mah FS, Dunn SP. (2019) American Academy of Ophthalmology Preferred Practice Pattern Cornea and External Disease Panel. Corneal Ectasia Preferred Practice Pattern®. *Ophthalmology*. 126: P170-P215.
26. Geiser MH, Bonvin M, Quibel O. (2004) [Corneal and retinal temperatures under various ambient conditions: a model and experimental approach.] *Klin Monatsbl Augenheilkd*, 221:311–314.
27. Gipson IK, Argüeso P, Beuerman R, Bonini S, Butovich I, Dana R, Dartt D, Gamache D, Ham B, Jumblatt M. (2007) Research in dry eye: report of the Research Subcommittee of the International Dry Eye WorkShop. *Ocular Surface* 5:179-193.
28. Goebels S, Eppig T, Seitz B, Szentmáry N, Cayless A, Langenbucher A. (2018) Endothelial alterations in 712 keratoconus patients. *Acta Ophthalmol*, 96:1134-1139.
29. Gregoratos ND, Bartsocas CS, Papas K. (1971) Blue sclerae with keratoglobus and brittle cornea. *Br J Ophthalmol*, 55:424–426.
30. Gugleta K, Orgül S, Flammer J. (1999) Is corneal temperature correlated with blood-flow velocity in the ophthalmic artery? *Curr Eye Res*, 19:496-501.
31. Guthoff RF, Wienss H, Hahnel C, Wree A. (2005) Epithelial innervation of human cornea: a three-dimensional study using confocal laser scanning fluorescence microscopy. *Cornea*, 24 (5):608–613.
32. Hara Y, Shiraishi A, Yamaguchi M, Kawasaki S, Uno T, Ohashi Y. (2014) Evaluation of allergic conjunctivitis by thermography. *Ophthalmic Res*, 51 (3):161–166.
33. Harding JR. (1998) Investigating deep venous thrombosis with infrared imaging. *IEEE Eng Med Biol Mag*, 17:43–46.
34. Hatwar R, Herman C. (2017) Inverse method for quantitative characterisation of breast tumours from surface temperature data. *Int J Hyperthermia*, 33:741–757.
35. Huff JW, Green K. (1981) Demonstration of active sodium transport across the isolated rabbit corneal endothelium. *Curr Eye Res*, 1:13–114.
36. Jacobs DS, Green WR, Maumenee AE. (1974) Acquired keratoglobus. *Am J Ophthalmol*, 77 (3):393–399.

37. Johnson RD, Nguyen MT, Lee N, Hamilton DR. (2011) Corneal biomechanical properties in normal, forme fruste keratoconus, and manifest keratoconus after statistical correction for potentially confounding factors. *Cornea*, 30 (5):516-23.
38. Kamao T, Yamaguchi M, Kawasaki S, Mizoue S, Shiraishi A, Ohashi Y. (2011) Screening for dry eye with newly developed ocular surface thermographer. *Am J Ophthalmol*, 151 (5):782–791.
39. Karabatsas CH, Cook SD. (1996) Topographic analysis in pellucid marginal corneal degeneration and keratoglobus. *Eye*, 10:451–455.
40. Kawali AA. (2013) Thermography in ocular inflammation. *Indian J Radiol Imaging*, 23: 281–283.
41. Kawasaki S, Mizoue S, Yamaguchi M, Shiraishi A, Zheng X, Hayashi Y, Ohashi Y. (2009) Evaluation of filtering bleb function by thermography. *Br J Ophthalmol*, 93:1331–1336.
42. Kennedy RH, Bourne WM, Dyer JA. (1986) A 48-year clinical and epidemiologic study of keratoconus. *Am J Ophthalmol*, 101:267– 273.
43. Kenney MC, Brown DJ. (2003) The cascade hypothesis of keratoconus. *Contact Lens Anterior Eye*, 26:139–146.
44. Kessel L, Johnson L, Arvidsson H, Larsen M. (2010) The relationship between body and ambient temperature and corneal temperature. *Invest Ophthalmol Vis Sci*, 51 (12):6593–6597.
45. Kheirkhah A, Saboo US, Abud TB, Dohlman TH, Arnoldner MA, Hamrah P, Dana R. (2015) Reduced corneal endothelial cell density in patients with dry eye disease. *Am J Ophthalmol*, 159:1022-1026.
46. Kitazawa K, Itoi M, Yokota I, Wakimasu K, Cho Y, Nakamura Y, Hieda O, Kinoshita S, Sotozono C. (2018) Involvement of anterior and posterior corneal surface area imbalance in the pathological change of keratoconus. *Sci Rep*, 8:14993.
47. Klamann MK, Maier AK, Gonnermann J, Klein JP, Bertelmann E, Pleyer U. (2013) Ocular surface temperature gradient is increased in eyes with bacterial corneal ulcers. *Ophthalmic Res*, 49:52–56.
48. Koenekoop RK. (2004) An overview of Leber congenital amaurosis: a model to understand human retinal development. *Surv Ophthalmol*, 49 (4):379–398.

49. Kolozsvári BL, Petrovski G, Gogolák P, Rajnavölgyi É, Tóth F, Berta A, Fodor M. (2014) Association between mediators in the tear fluid and the severity of keratoconus. *Ophthalmic Res*, 51 (1):46–51.
50. Konieczka K, Schoetzau A, Koch S, Hauenstein D, Flammer J. (2018) Cornea thermography: optimal evaluation of the outcome and the resulting reproducibility. *Transl Vis Sci Technol*, 7:14.
51. Langenbucher A, Seitz B, Nguyen NX, Naumann GOH. (2002) Corneal endothelial cell loss after nonmechanical penetrating keratoplasty depends on diagnosis: a regression analysis. *Graefes Arch Clin Exp Ophthalmol*, 240: 387–392.
52. Lasanen R, Piippo-Savolainen E, Remes-Pakarinen T, Kröger L, Heikkilä A, Julkunen P, Karhu J, Töyräs J. (2015) Thermal imaging in screening of joint inflammation and rheumatoid arthritis in children. *Physiol Meas*, 36(2):273-82.
53. Lema I, Sobrino T, Duran JA, Brea D, Díez-Feijoo E. (2009) Subclinical keratoconus and inflammatory molecules from tears. *Br J Ophthalmol*, 93:820–824.
54. Luchs JI, Cohen EJ, Rapuano CJ, Laibson PR. (1997) Ulcerative keratitis in bullous keratopathy. *Ophthalmology*, 104: 816–822.
55. Määttä M, Heljasvaara R, Sormunen R, Pihlajaniemi T, Autio-Harmainen H, Tervo T. (2006) Differential expression of collagen types XVIII/endostatin and XV in normal, keratoconus and scarred human corneas. *Cornea*, 25:341–349.
56. Määttä M, Väisänen T, Väisänen MR, Pihlajaniemi T, Tervo T. (2006) Altered expression of type XIII collagen in keratoconus and scarred human corneas: increased expression in scarred cornea is associated with myofibroblast transformation. *Cornea*, 25:448–453.
57. Mandathara PS, Stapleton FJ, Kokkinakis J, Willcox MDP. (2018) A pilot study on corneal Langerhans cells in keratoconus. *Cont Lens Anterior Eye*, 41:219–223.
58. Mapstone R. (1968) Corneal thermal patterns in anterior uveitis. *Br J Ophthalmol*, 52:917–921.
59. Mapstone R. (1968) Determinants of corneal temperature. *Br J Ophthalmol*, 52:729–741.

60. Mapstone R. (1970) Ocular thermography. *Br J Ophthalmol*, 54:751–754.
61. Mathews PM, Ramulu PY, Friedman DS, Utine CA, Akpek EK. (2013) Evaluation of ocular surface disease in patients with glaucoma. *Ophthalmology*, 120:2241-8.
62. McDonald JM, Geroski DH, Edelhauser HF. (1987) Effect of inflammation on the corneal endothelial pump and barrier. *Curr Eye Res*, 6:1125–1132.
63. Mergler S, Pleyer U. (2007) The human corneal endothelium: new insights into electrophysiology and ion channels. *Prog Retin Eye Res*, 26:359-378.
64. Morgan P. (1994) Ocular thermography in health and disease. Manchester; Ph.D. thesis.
65. Morgan PB, Tullo AB, Efron N. (1995) Infrared thermography of the tear film in dry eye. *Eye*, 9:615–618.
66. Moussa S, Eppig T, Pattmöller J, Zemova E, Seitz B, Langenbucher A, Szentmáry N. (2013) Diurnal and zonal analysis of corneal surface temperature in young healthy adults. *Eur J Ophthalmol*, 5: 641-645.
67. Muller LJ, Pels L, Vrensen GF. (1996) Ultrastructural organization of human corneal nerves. *Invest Ophthalmol Vis Sci*, 37:476–488
68. Nelson ME, Talbot JF. (1989) Keratoglobus in Rubinstein-Taybi syndrome. *Br J Ophthalmol*, 73:385–387.
69. Németh O, Langenbucher A, Eppig T, Lepper S, Milioti G, Abdin A, Nagy ZZ, Seitz B, Szentmáry N. (2020a) Ocular Surface Disease Index and Ocular Thermography in Keratoconus Patients. *J Ophthalmol*, 8; 2020:1571283.
70. Németh O, Langenbucher A, Eppig T, Lepper S, Milioti G, Abdin A, Nagy ZZ, Seitz B, Szentmáry N. (2020b) Correlation between Corneal Endothelial Cell Density and Central Ocular Surface Temperature in Normal and Keratoconus Eyes. *Curr Eye Res*. 27:1-7.
71. Németh O, Lepper S, Milioti G, Abdin A, Seitz B, Eppig T, Langenbucher A, Nagy ZZ, Szentmáry N. (2020c) Ocular Surface Disease Index, biomechanical properties and ocular thermography in a keratoglobus patient. *Ophthalmologia Hungarica*, 157:231-237.

72. Niederer RL, Perumal D, Sherwin T, McGhee CNJ. (2007) Age-related differences in the normal human cornea: a laser scanning *in vivo* confocal microscopy study. *Br J Ophthalmol*, 91:1165–1169.
73. Nottingham J. (1984) Practical observations on conical cornea. London: Churchill, London, p. 1–19.
74. Oliveira-Soto L, Efron N. (2001) Morphology of corneal nerve using confocal microscopy. *Cornea*, 20:374–384
75. Pásztor D, Kolozsvári BL, Csutak A, Berta A, Hassan Z, Kettesy BA, Gogolák P, Fodor M. (2016) Scheimpflug Imaging Parameters Associated with Tear Mediators and Bronchial Asthma in Keratoconus. *J Ophthalmol*, 2016:9392640.
76. Pattmöller J, Wang J, Zemova E, Seitz B, Eppig T, Langenbucher A, Szentmáry N. (2015) Correlation of corneal thickness, endothelial cell density and anterior chamber depth with ocular surface temperature in normal subjects. *Z Med Phys*, 25:243-250.
77. Pattmöller M, Wang J, Pattmöller J, Zemova E, Eppig T, Seitz B, Szentmáry N, Langenbucher A. (2015) [Interobserver and intraobserver reliability of corneal surface temperature measurements with the TG-1000 thermograph in normal eyes]. *Ophthalmologe*, 112: 746-751.
78. Pouliquen Y, Dhermy P, Espinasse MA, Savoldelli M. (1985) Keratoglobus. *J Fr Ophthalmol*, 8:43–45.
79. Pricopie S, Istrate S, Voinea L, Leasu C, Paun V, Radu C. (2017) Pseudophakic bullous keratopathy. *Rom J Ophthalmol*, 61:90-94.
80. Purslow C, Wolffsohn J. (2007) The relation between physical properties of the anterior eye and ocular surface temperature. *Optom Vis Sci*, 84:197-201.
81. Purslow C, Wolffsohn JS. (2005) Ocular surface temperature: a review. *Eye Contact Lens*, 31: 117– 123.
82. Rabinowitz YS. (1998) Keratoconus. *Surv Ophthalmol*, 42:297–319.
83. Reinhard T, Böhringer D, Sundmacher R. (2001) Accelerated chronic endothelial cell loss after penetrating keratoplasty in glaucoma eyes. *J Glaucoma*, 10: 446–451.

84. Saito A, Kamiya K, Fujimura F, Takahashi M, Shoji N. (2020) Comparison of angle-to-angle distance using three devices in normal eyes. *Eye (Lond)*, 34:1116-1120.
85. Schroeter J, Meltendorf C, Ohrloff C, Rieck P. (2008) Influence of temporary hypothermia on corneal endothelial cell density during organ culture preservation. *Graefes Arch Clin Exp Ophthalmol* 246:369-372.
86. Schroeter J, Ruggeri A, Thieme H, Meltendorf C. (2015) Impact of temporary hyperthermia on corneal endothelial cell survival during organ culture preservation. *Graefes Arch Clin Exp Ophthalmol* 253:753-758.
87. Slettedal JK, Ringvold A. (2015) Correlation between corneal and ambient temperature with particular focus on polar conditions. *Acta Ophthalmol*, 93: 422–426
88. Sniegowski MC, Erlanger M, Olson J. (2018) Thermal imaging of corneal transplant rejection. *Int Ophthalmol*, 38:2335-2339.
89. Stachon T, Kolev K, Flaskó Z, Seitz B, Langenbucher A, Szentháry N. (2017) Arginase activity, urea, and hydroxyproline concentration are reduced in keratoconus keratocytes. *Graefes Arch Clin Exp Ophthalmol*, 255:91-97.
90. Stachon T, Latta L, Kolev K, Seitz B, Langenbucher A, Szentháry N. (2019) [Increased NF-κB and iNOS expression in keratoconus keratocytes - hints for an inflammatory component?] *Klin Monbl Augenheilkd*. 2019 Oct 10. doi: 10.1055/a-1002-0100. Online ahead of print.
91. Stachon T, Stachon A, Hartmann U, Seitz B, Langenbucher A, Szentháry N. (2017) Urea, uric acid, prolactin and fT4 concentrations in aqueous humor of keratoconus patients. *Curr Eye Res*, 42:842-846.
92. Su TY, Ho WT, Chiang SC, Lu CY, Chiang HK, Chang SW. (2017) Infrared thermography in the evaluation of meibomian gland dysfunction. *J Formos Med Assoc*, 116:554-559.
93. Tepelus TC, Chiu GB, Huang J, Huang P, Sadda SR, Irvine J, Lee OL. Correlation between corneal innervation and inflammation evaluated with confocal microscopy and symptomatology in patients with dry eye syndromes: a preliminary study. (2017) *Graefes Arch Clin Exp Ophthalmol*, 255:1771-1778.

94. Tervo T, Palkama, A. (1975) Electron microscopic localization of adenosine triphosphatase (NaK-ATPase) activity in the rat cornea. *Exp Eye Res*, 21, 269–279.
95. Uçakhan OO, Kanpolat A, Ylmaz N, Ozkan M. (2006) In vivo confocal microscopy findings in keratoconus. *Eye Contact Lens*, 32:183–191.
96. Verrey F. (1947) Keratoglobe aigu. *Ophthalmologica*, 114:284–288.
97. Vinciguerra R, Ambrósio R Jr, Elsheikh A, Roberts CJ, Lopes B, Morenghi E, Azzolini C, Vinciguerra P. (2016) Detection of Keratoconus With a New Biomechanical Index. *J Refract Surg*, 1;32:803-810.
98. Wallang BS, Das S. (2013) Keratoglobus. *Eye*, 27:1004-1012.
99. Walt J. (2004) Ocular Surface Disease Index (OSDI) Administration and Scoring Manual. Irvine, CA: Allergan, Inc.
100. Weed KH, MacEwen CJ, Giles T, Low J, McGhee CN. (2008) The Dundee University Scottish Keratoconus study: demographics, corneal signs, associated diseases, and eye rubbing. *Eye (Lond)*, 22:534–541.
101. Yamaguchi T, Higa K, Suzuki T, Nakayama N, Yagi-Yaguchi Y, Dogru M, Satake Y, Shimazaki J. (2016) Elevated cytokine levels in the aqueous humor of eyes with bullous keratopathy and low endothelial cell density. *Invest Ophthalmol Vis Sci*, 57: 5954-5962.
102. Zarnowski T, Lekawa A, Dyduch A, Turek R, Zagórski Z. (2005) [Corneal endothelial density in glaucoma patients]. *Klin Oczna*, 107:448-451.
103. Zemova E, Eppig T, Seitz B, Toropygin S, Arnold S, Langenbucher A, Gräber S, Szentmáry N. (2014) Interaction between topographic/tomographic parameters and dry eye disease in keratoconus patients. *Curr Eye Res*, 39:1-8.
104. Zhivov A, Stave J, Vollmar B, Guthoff R. (2005) In vivo confocal microscopic evaluation of Langerhans cell density and distribution in the normal human corneal epithelium. *Graefes Arch Clin Exp Ophthalmol*, 243:1056–1061.
105. Zhivov A, Stave J, Vollmar B, Guthoff R. (2007) In vivo confocal microscopic evaluation of langerhans cell density and distribution in the corneal epithelium of healthy volunteers and contact lens wearers. *Cornea*, 26:47–54.

9. Bibliography

9.1 Thesis related publications

Original articles

1. Németh O, Langenbucher A, Eppig T, Lepper S, Milioti G, Abdin A, Nagy ZZ, Seitz B, Szentmáry N. Ocular Surface Disease Index and ocular thermography in keratoconus patients. *J Ophthalmol* 2020; epub |Article ID 1571283 **IF: 1.580**
2. Németh O, Langenbucher A, Eppig T, Lepper S, Milioti G, Abdin A, Nagy ZZ, Seitz B, Szentmáry N. Correlation between corneal endothelial cell density and central corneal temperature in normal and keratoconus eyes. *Curr Eye Res* 2020 Aug 27:1-7. doi: 10.1080/02713683.2020.1812087. Online ahead of print. **IF: 1.754**
3. Németh O, Lepper S, Milioti G, Abdin A, Seitz B, Eppig T, Langenbucher A, Nagy ZZ, Szentmáry N. Ocular Surface Disease Index, biomechanical properties and ocular thermography in a keratoglobus patient. *Ophthalmologia Hungarica* 2020; 157:231-237.

9.2 Other publication

Original articles

1. Németh O, Bátor G. [The classification of ocular trauma cases between 2014 and 2018 at the in-patient ophthalmological department of the Markusovszky University Teaching Hospital]. *Orv Hetil* 2019; 160: 1941–1947. **IF: 0.564**
4. Tóth G, Pluzsik M, Sándor LG, Németh O, Lukáts O, Nagy ZZ, Szentmáry N. Clinical review of microbial corneal ulcers resulting in enucleation and evisceration in a tertiary eye care center in Hungary. *J Ophthalmol* 2020 May 18; 2020: 8283131. doi: 10.1155/2020/8283131. eCollection 2020. **IF: 1.580**
2. Pluzsik MT, Tóth G, Németh O, Kerényi Á, Nagy ZZ, Szentmáry N. Introduction of posterior lamellar keratoplasty techniques at the Department of Ophthalmology of Semmelweis University; effect on number of keratoplasties and penetrating

keratoplasties due to corneal decompensation between 2008 and 2017. Ophthalmologia Hungarica, 2020; 157:36-41.

Case reports

1. Németh O, Zsidegh P, Szigeti A, Tapasztó B, Nagy ZZ, Maka E. Bilateral progressive myopia and dislocation of the lens in childhood: A case of homocystinuria. Case report. Ophthalmologia Hungarica 2017; 154: 148-153.
2. Németh O, Farkas K, Tóth É, Tóth B, Nagy ZZ, Resch M. Ophthalmic side effect of the systemic MEK inhibitor therapy in the case of melanoma malignum – Case report. Ophthalmologia Hungarica 2017; 154: 154-157.

Review article

1. Németh O, Tapasztó B, Tar S, Szabó V, Nagy ZZ, Tóth J, Hamed A, Mikala G, Szentmáry N. [Corneal deposits in monoclonal gammopathy of undetermined significance. Review of the literature and case report]. Orv Hetil 2018; 159: 1575-1583. **IF: 0.564**

10. Acknowledgements

Foremost, I would like to thank my supervisor Prof. Dr. Nóra Szentmáry for the continuous support of my doctoral study and research, for her patience, motivation, enthusiasm, and immense knowledge. Her guidance helped me all the time of research and writing of this thesis. I could not have imagined having a better advisor and mentor for my PhD study.

Besides my supervisor, I would like to thank Prof. Dr. Achim Langenbucher, Prof. Dr. Berthold Seitz and Prof. Dr. Zoltán Zsolt Nagy for their encouragement, their insightful comments and hard questions.

I would also like to thank Prof. Dr. Achim Langenbucher for the comprehensive statistical analysis of our huge dataset.

My sincere thanks also go to Prof. Dr. Berthold Seitz and Dr. György Bátor, for the opportunity of the three months long internship in Homburg/Saar, Germany. I thank all my co-authors, Prof. Dr. Timo Eppig, Dr. Sabine Lepper, Dr. Georgia Milioti, Dr. Alaa Din Abdin for all their support during the whole research.

I would also like to thank for the support of all colleagues at the Department of Ophthalmology, Semmelweis University, Budapest, Hungary, at the Department of Ophthalmology, Saarland University Medical Centre, Homburg/Saar, Germany, at the Experimental Ophthalmology, Saarland University, Homburg/Saar, Germany and at the Department of Ophthalmology of the Markusovszky University Teaching Hospital, Szombathely, Hungary.

I thank for the grant of the European Board of Ophthalmology (EBO Travel Grant), as my main financial support in my research stay in Homburg/Saar. I also would like to acknowledge the HARVO, for its support in presentation of our research at the ARVO Congress, in 2019.

Special thanks for for the stimulating discussions with my “PhD-friends”, Dr. Milán Tamás Pluzsik and Dr. Gábor Tóth. Finally, I would like to thank my family and my beloved fiancé for their encouragement, their insightful comments and for their patience during this difficult, exciting and challenging period of our lives.